8-2022

Characterization of Genetic Pathways Involved in Resistance to a Novel Antifungal Peptide

Kayla L. Haberman
University of Arkansas, Fayetteville

Characterization of Genetic Pathways Involved in Resistance to a Novel Antifungal Peptide

A Thesis submitted in partial fulfillment
of the requirements for the degree of
Master of Science in Cell and Molecular Biology

by

Kayla L. Haberman
Ouachita Baptist University
Bachelor of Science in Biology & Psychology, 2020

August 2022
University of Arkansas

This thesis is approved for recommendation to the Graduate Committee

_____
Inés Pinto, Ph.D.
Major Professor

_____
Jeffrey A. Lewis, Ph.D.
Committee Member

_____
Josh Sakon, Ph.D.
Committee Member

ABSTRACT

Antibiotic resistance is increasing prevalence, particularly in *Candida glabrata*. This opportunistic pathogen is closely phylogenetically related to *Saccharomyces cerevisiae;* however, its characterization is limited. *C. glabrata* is only second to *Candida albicans* as a fungal pathogen in immunocompromised patients. Commonly resistant to azoles, the most common fungal therapy, it has become costly and challenging to treat. A histatin 5 derived antifungal peptide, KM29, has a high degree of efficacy in *Candida* species and *S. cerevisiae*. The objective of this work is to advance our understanding of the mechanism of action of KM29 against *C. glabrata*. Previous work in the lab used the *S. cerevisiae* deletion library as a related fungal system to identify mutants that resulted in increased resistance to KM29, with the goal of discovering pathways that could then be tested in *C. glabrata*. In this work we focused on plasma membrane transporters identified in the *S. cerevisiae* screen. Validation of the KM29 killing activity showed no significant increased resistance in deletions of four hexose transporters (*HXT2*, *HXT3*, *HXT5*, and *HXT10*) or two metal transporters (*FET4* and *ZRT2*). Deletion of the membrane sterol regulator *LAM1* and its paralog *SIP3* showed significant resistance to KM29, as well as the polyamine transporter *AGP2*. We concentrated on setting up the CRISPR-Cas9 system to delete *C. glabrata AGP2*. A successful deletion was confirmed by DNA sequencing and positive mutants displayed increased resistance to KM29 in *C. glabrata***,** although no increased resistance to polyamine toxicity was observed. Further analyses are needed to investigate *AGP2* function. We conclude that the screen in *S. cerevisiae* can be useful to identify pathways in *C. glabrata* to understand the fungicidal mechanism of KM29.

ACKNOWLEDGEMENTS

I would like to express my gratitude to Dr. Inés Pinto for adding me to her research team during the COVID pandemic. Her guidance has sparked an interest to continue developing and improving my ability as a researcher. She has provided me with equipment, materials, and direction throughout the duration of this project, and my time at the University of Arkansas. I would like to thank the Dr. David McNabb for his support and providing background information regarding the creation of KM29. Thank you to Allison McFarland, in Dr. Tipsmark's lab, for her sustained help troubleshooting and being a dear friend in lab. Thank you, Richard Wells, for your interest in the lab and continuing aspects of my research. I would like to thank Joshua, Sean, many other friends, and family members for their constant support while I pursued my master's degree.

'With God, all things are possible.' - Matthew 19:26

TABLE OF CONTENTS

INTRODUCTION

C. glabrata has become increasingly prominent as the causative agent of fungal infections in immunosuppressed patients, leading to high morbidity and mortality, and costly treatments. Although related closer phylogenetically to the baker's yeast, *S. cerevisiae*, than to the other pathogenic Candida species, it presents distinct features that make it a particularly dangerous pathogen. *C. glabrata* is commonly resistant to azoles, the first line of antifungal drugs, and becomes easily resistant to echinocandins, the standard drug for *C. glabrata* infections. Previous work aimed at understanding the mode of action of a novel antifungal peptide, KM29, a derivative of the natural antimicrobial histatin 5, involved the screening of the whole genome deletion collection in *S. cerevisiae* (Bullock et al. 2020). The outcome provided information about many genes and pathways potentially relevant for the fungicidal activity of KM29 against *Candida* species. This preliminary work proved the importance of mitochondrial function in the killing activity of KM29 in *S. cerevisiae* and *C. albicans* and identified many other pathways that required further analysis. The work presented here focuses on the validation of mutations in various plasma membrane transporters identified in *S. cerevisiae*, and the establishment of the CRISPR-Cas9 system in *C. glabrata* to delete the homolog genes and characterize their involvement in the fungicidal activity of KM29 in this opportunistic pathogen.

1.1 Candidiasis

Fungi comprise over 120,000 classified types including mushrooms, yeast, lichens, rust, and mold. Fungi can be a valuable nutrient source, are used to create vaccines, consume toxic chemicals to eliminate from the environment, and more uses are being discovered daily (Camu 2019). Fungi can be harmful to vegetation and living organisms by causing disease and death. Fungal infections have become more prevalent in society today, becoming a leading major health concern. Fungal infections caused by yeast, typically in the oral or vaginal cavities, lead to candidiasis, an opportunistic infection. In cases of immunocompromised people (for example cancer, transplant, or HIV patients) yeast infections can drastically exacerbate health conditions.

Candida has evolved to be opportunistic pathogens, which can be evolutionarily driven by adaption to the host environment (Schwarzmüller et al. 2014).

Candidemia, a bloodstream infection from yeast, is a common infection in hospitalized patients (Invasive Candidiasis 2020). Candida bloodstream infections are the second most common pathogen causing hospitalizations (Mazi et al. 2022) and are often a financial burden if treatment is received (Morgan et al. 2005). Candida can enter the bloodstream from one of three identified routes: gastrointestinal tract mucosal barrier, intravascular catheter, and a localized infection (R. AN, et al. 2022). Approximately 65% of infected people receive treatment for approximately seven days, with the estimated the cost to treat in the United States being $44 million to $320 million annually (Morgan et al. 2005). Candida infections have a mortality range of 19% - 24% for people in the United States. (Morgan et al. 2005) with 90-day crude mortality of 42.4% for Candida bloodstream infections (Mazi et al. 2022). Candida bloodstream infections are often mischaracterized, accounting for 91% of untreated cases, causing a significant increase in mortality (Mazi et al. 2022), due to improper treatment.

Candida species can affect the oral cavity and genitals and include *C. albicans*, *C. glabrata*, *C. krusei*, *C. parapsilosis*, *C. pseudotropicalis*, *C. stellatoidea*, and *C. tropicalis* (R. AN, et al. 2022). An oral candida infection is known as thrush and appears as a white or yellow non-scrapable rash on the tongue and mucous membranes of the mouth, or redness and soreness with cracking at the corners of the mouth (R. AN, et al. 2022). Vaginal candidiasis presents with genital itching, burning, and a white "cottage cheese-like" discharge from the vagina (R. AN, et al. 2022). Vulvovaginal mucosal infections are common in women who get urinary tract infections and in babies in the form of diaper rash. Prevalence of vulvovaginal candidiasis (VVC) in pregnant women is an increasing trend in our community (Ghaddar et al. 2019) and can cause low birth weight if treated with the incorrect anti-fungal. Systemic candidemia causes fever, chills, hypotension, and confusion (R. AN, et al. 2022), and can cause serious damage to internal organs and bodily function. The chances of candida infections in pregnant women

increase through pregnancy; due to the hormonal changes resulting in high levels of estrogens, progesterone, and corticosteroids which decrease the natural immune response (Ghaddar et al. 2019).

1.2 Saccharomycotina

Saccharomycotina is a sub phylum of the Ascomycota phylum and are known to be the "true yeasts" (Mueller et al. 2004) and species of this class share a large portion of genes. They are a monophyletic clade with-the most recent ancestor believed to be Euascomyetes (Mueller et al. 2004). This group of yeast is associated with food in the form of baker's yeast or as a pathogen to mammals (Mueller et al. 2004). A major difference between species within this subphylum is the whole-genome duplication (WGD) clade and the CTG clade that codes CUG to serine in *Candida* species (Roetzer et al. 2010). The CTG clade is known to house pathogenic yeast such as *C. albicans* while the WGD clade contains both *S. cerevisiae* and *C. glabrata*. WGD eventually lost the duplicated portion of genes; however, it had molecular consequences since many genes were deleted and increased the evolution timeline (Kurtzman et al. 2011). This resulted in some genes only having a paralog and not an ortholog; however, in *S. cerevisiae* it is found to have many orthologs in *C. glabrata*. These two genomes show far more shared losses of genes and have shared rearrangements throughout the genome (Kurtzman et al. 2011) compared to other species.

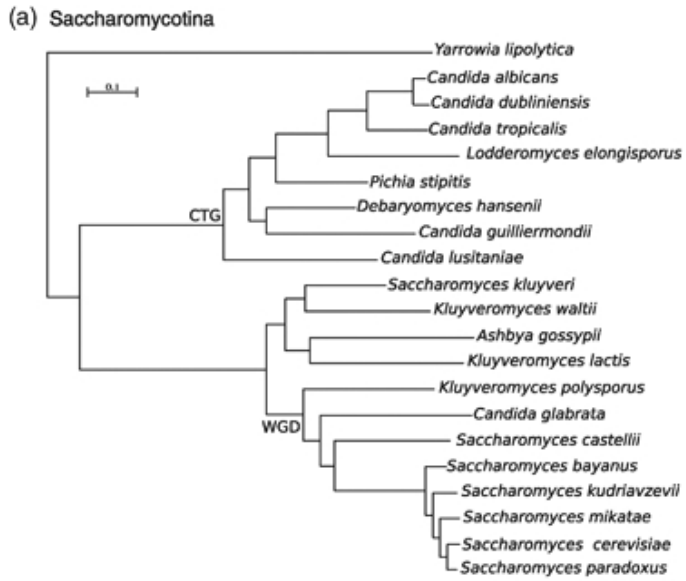

Figure A: Adapted from Roetzer, A., Gabaldón, T., & Schüller, C. (2010). From Saccharomyces cerevisiae to Candida glabrata in a few easy steps: important adaptations for an opportunistic pathogen. *FEMS Microbiology Letters*, *314*(1), 1–9. https://doi.org/10.1111/j.1574-6968.2010.02102.x

1.1.1 Saccharomyces cerevisiae

Saccharomyces cerevisiae is one of the most comprehensively and accurately sequenced species in existence (Kurtzman et al. 2011). Known as baker's yeast, it is capable of vegetative and sexual reproduction. Through nitrogen starvation, diploid *S. cerevisiae* switch to pseudohyphal growth (Csank & Haynes, 2000) meiosis forming ascospores that are stress-resistant, while haploid *S. cerevisiae* forms invasive pseudohyphal growth on rich media.

S. cerevisiae cell wall is composed of glycosylphosphatidylinositol-linked flocculins (FLO) which is involved in biofilm formation and cell adhesion (Roetzer et al. 2010). Another important aspect of *S. cerevisiae* is the plasma membrane that is involved in and regulates major biological processes, such as establishing and maintaining transmembrane gradients, controlling uptake and secretion, cellular communication, and recognition (Ferraz et al. 2021). Membrane-bound proteins ABC (ATP binding cassette) are a important part of the membrane since they are involved in the uptake of amino acids, peptides, and sugar (Kumar R. et al 2011). They act as

gate or ion channels and regulate most transport processes within the cell. Another important part of the membrane are the polyamine transport, which is regulated by the GAP family members. GAP members are found to regulated in response to antifungal drugs: ketoconazole, caspofungin, flucytosine (Kumar R. et al 2011). The plasma membrane is also affected by the H^+ drug antiporter subfamily, which catalyzes the transport of polyamines at the plasma membrane level (Aouida et al. 2005). The genes coding for transporters are important to analyze as they offer a mode of action for various antifungals. Observing the effect in *S. cerevisiae* will be a template for analysis in *C. glabrata*.

1.1.2 Candida Glabrata

Candida glabrata is very similar to *S. cerevisiae* except it lacks a sexual cycle, must undergo vegetative reproduction to regenerate, thrives at a higher temperature, and does not demonstrate filamentous growth (Csank & Haynes, 2000). *C. glabrata* is very small in size, has a rapid growth rate, a short regeneration time, is able to produce a biofilm, and grows best at 37ºC, which is why it thrives as a human commensal (Roetzer et al. 2010). DNA analysis demonstrates the sequence similarity between *S. cerevisiae* and *C. glabrata* (Csank &Haynes,-2000), This makes *C. glabrata* more phylogenetically related to *S. cerevisiae* than *C. albicans*. *C. glabrata* is a opportunistic pathogenic yeast like *C. albicans* and they belong to the same genus (Raschmanová et al 2018) but *C. glabrata* belongs to the WGD clade while *C. albicans* belongs to the CTG clade. *C. glabrata* is a part of humans' natural flora; however, it-can quickly become a severe health threat (Schwarzmüller et al. 2014). In fungal pathogens, the lack of a sexual cycle is common (Roetzer et al. 2010) which allows the formation of resistant spores. Due to *C. glabrata* being a haploid fungal pathogen, it is a good model organism for analysis of its fungal virulence (Csank & Haynes, 2000). *C. glabrata* is found to secrete yapsin proteases which are important for pathogenicity; without yapsin protease, macrophage survival is reduced (Bullock 2018).

C. glabrata is not known to penetrate tissues, but instead creates a biofilm on mucosal surfaces (Roetzer et al. 2010). The production of silent adhesion-genes of the EPA family and other adhesion genes provides *C. glabrata* many opportunities to form biofilms on a wide variety of surfaces (de Groot et al. 2008). Biofilm formation has been linked to increased resistance toward antimicrobial peptides. *C. glabrata* has demonstrated an inherent tolerance to azole drugs, becoming a serious clinical threat and complicating therapeutic management (Schwarzmüller et al. 2014). Research has demonstrated azole resistance is often due to enhanced drug efflux which is caused by overexpression of ATP-binding cassette transporter genes (Tati et al. 2013).

Behind *C. albicans*, *C. glabrata* is the most common cause of vaginal and oral candidiasis, becoming an important candida species in the United States (Roetzer et al. 2010). Being the second most common cause of candidemia in the world with a higher level of intrinsic azole resistance than C. *albicans* (Pais et al. 2016), it accounts for 15-20% of all candida infections (Roetzer et al. 2010 & Schwarzmüller et al. 2014). Not only can it thrive on mammalian cells, but it can live up to five months on surfaces, which is one month longer than *C. albicans* (Roetzer et al. 2010) is known to survive.

Many *S. cerevisiae* orthologs are found in *C. glabrata* and the gene order between the two species is highly conserved (Roetzer et al. 2010); however, *C. glabrata* shows a higher rate of gene loss from common ancestor than *S. cerevisiae*. *C. glabrata* lacks genes of galactose, phosphate, nitrogen, and sulfur metabolism (Roetzer et al. 2010) and relies on the host or environment for its auxotrophic needs. A unique aspect of *C. Glabrata's* genome is megasatellites, which are repetitive sequences encoding for cell-wall proteins and thought to be related to high degree of plasticity (Roetzer et al. 2010). Megasatellightes have been found to encode glycosylphosphatidylinositol-linked epithelial adhesion (EPA) genes, encoding for non-hyphae specific adhesions (Bullock 2018). EPA genes are thought to have diverged in evolutionary sequence from *S. cerevisiae* FLO genes; they contain tandem repeats approximately

the same length and found in subtelomeric regions. FLO and EPA genes functions are similar however the genome had diverged beyond sequence recognition (Roetzer et al. 2010).

C. glabrata has another unique feature of higher surface levels of β-1,3-glucans when compared with *C. albicans*; however, this does not account for reduced Histatin-5 (Hst5) uptake, killing, nor biofilm formation (Tati et al. 2013). *C. glabrata* also has a higher mannose/glucose ratio and 50% more mannoprotein incorporated into the cell wall compared to *S. cerevisiae* and *C. albicans* (de Groot et al. 2008) which can contribute to its unique adhesion abilities.

1.2 Current Antifungal Therapies

Current treatment of fungal infections is limited to three classes of compounds: polyenes, echinocandins, and azoles. Most antifungals have drug-drug interaction that is harmful to the patient, which stresses the importance to properly diagnose the condition before selecting a treatment method. Treatments consist of an oral medication or topical ointment; both being highly effective. A major difference between the two is the cost to produce and cost to consumer. Oral medication is very expensive and typically a one-time dose in comparison to antifungal creams which are affordable and come in 1, 3, or 7-day treatment (R. AN, et al. 2022).

1.2.1 Polyenes

Polyenes were the first class of antifungals to be discovered. They act with a broad-spectrum targeting ergosterol in the cell wall (Perea & Patterson, 2002). This class functions by binding to ergosterol, and alter membrane function (Perea & Patterson, 2002) by creating pores in the membrane causing in cell death (Bullock 2018). Amphotericin B deoxycholate, a broad-spectrum polyene, is the only polyene compound clinically approved to treat candida infections (Bullock 2018). It appears to cause a change in the amount of ergosterol in the cell membrane (Perea & Patterson, 2002) altering the fluidity. Against *Candida* species, the minimal inhibiting concentration (MIC_{90}) for Amphotericin B (AmB) ranges from 0.12-4 (Bullock 2018). Enhanced affinity has been found for of AmB for ergosterol due to specific complexes formed ~~d~~on the

membrane (Neumann et al 2010). It has been found that sterol transporters are essential for Amp B due to membrane association (Neumann et al 2010). Amphotericin B does not have and major drug-drug interactions, however it has been known to induce renal toxicity and damage (Bullock 2018). Synthetic amphotericin B has been created to decrease cost and the addition of lipids have demonstrated a decrease toxicity, but the cost of production is very high (Bullock 2018). This has not demonstrated a clear advantage (Perea & Patterson, 2002) resulting in amphotericin B the most effective polyene.

1.2.2 Echinocandins

Echinocandins are semisynthetic lipopeptides (Bullock 2018) and a newer class of antifungals that are quite expensive (Schwarzmüller et al. 2014) to produce. They function by inhibiting the 1,3-β-D-glucan synthase, which is essential to cell wall of pathogenic yeast (Schwarzmüller et al. 2014 & Perea & Patterson, 2002). Echinocandins have a narrow spectrum and come with a few drug-drug interactions and toxicity issues (Bullock 2018). This class is also known for treatment of blood stream infection caused by candida due to its function. The three compounds in this class include caspofungin, micafungin, anidulafungin, which are all an effective treatment against *candida* with MIC_{90} values ranging from 0.03-4 (Bullock 2018). Echinocandins have shown to be as effective as amphotericin B and fluconazole with fewer adverse effects (Bullock 2018). -This has shifted the treatment away from fluconazole and to echinocandins instead (Bullock 2018).

1.2.3 Azole

Azoles are known for their five-membered aromatic rings containing nitrogen atoms (Bullock 2018). Azoles are a family of compounds including triazoles, commonly-treating systemic infections, and imidazole, such as trimazole, commonly treating superficial infections (Pais et al. 2016). Azoles activate ergosterol biosynthesis which is essential for the cell wall (Perea & Patterson, 2002). Major compounds in this class including fluconazole, itraconazole,

posaconazole, voriconazole. (Bullock 2018) Fluconazole and itraconazole are found to be effective against all fungal species except *C. glabrata* and *C. krusei*. (Bullock 2018); yet they are the most prescribed antifungals to treat *C. glabrata* which has led to its acquired resistance to this class of compounds (Bullock et al. 2020). Posaconazole has good activity against most Candida species (Bullock 2018) with rare and mild adverse effects. Other azoles are known to have toxic and negative interactions with medications including immunosuppressants, antiarrhythmics, antipsychotics, and migraine (Bullock 2018) which can cause life-threatening effects. Azoles have also been found to cause premature or low birth weight when prescribed to pregnant women, making amphotericin B is preferred (Bullock 2018) treatment for pregnant women due to lack of negative effects in pregnancy.

1.2.4 Antimicrobial peptides (AMP)

While synthesized peptides are useful, understanding naturally synthesized peptides provide a foundation to build from AMPs are the first natural line of defense against invading pathogens and are vital to the immune system (Bullock et al. 2020). Antimicrobial peptides (AMP) are found to have a variety of functions including antibacterial, antifungal, antiviral, and antitumor activities; all occurring through a variety of mechanisms such as membrane permeabilization, mitochondrial perturbations, initiation of apoptosis, osmotic stress, and DNA damage (Bullock et al. 2020). AMP are often cationic and amphiphilic peptides (Lei et al. 2019). AMP is found to interact with the negative charge on bacterial membranes and can penetrate membranes activating cellular damage (Lei et al. 2019). Naturally synthesized AMP are typically unstable, have a short half-life, and have severe hemolytic activity (Lei et al. 2019). Due to the short half-life, these molecules are constantly synthesized to maintain activity. Synthetic development AMP often has high toxicity with low activity and stability (Bullock 2018). Developing modified AMP can decrease the cost of production while increasing activity (Bullock 2018). For synthetic AMP, substitutions intended to increase hydrophobicity and/or cationicity improves activity, while the addition of bulky side chains improves (Bullock et al. 2020).

1.2.5 Histatin

Histatins are a group of antimicrobial peptides are cationic and histidine-rich peptides. These peptides range from 7 to 38 amino acid residues in length (Kavanagh & Dowd, 2004). It is interesting to note that despite natural variations, the charge on Histatin is like that of polyamines, positive (Kumar R. et al. 2011). Histatins are a group of antimicrobial peptides that are naturally synthesized in salivary glands and contain antifungal properties (Kavanagh & Dowd, 2004). This group functions by targeting the cell membrane, entering the cytoplasm, and targeting the mitochondria. To have the highest toxicity, it must translocate rapidly, and translocation is found to be decreased by low temperatures (Kavanaugh & Dowd, 2004). Upon entry to the cell, they cause G1 arrest, induce non-lytic loss of ATP from actively respiring cells and disrupt the cell cycle leading to the generation of reactive oxygen species (ROS) (Kavanagh & Dowd, 2004). Histatin is the most potent antimicrobial while-histatin--5 (Hst-5) is the only histatin with antifungal properties that is commonly found in body flora (Kavanagh & Dowd,2004). Higher levels of histatin are found in patients with reoccurring candidiasis along with associated lesions (Kavanagh & Dowd,).

Histatin-5 (D-S-H-A-K-R-H-H-G-Y-K-R-K-F-H-E-K-H-H-S-H-R-G-Y) is 24 amino acids in length with a functional domain for fungicidal activity found at the C-terminal domain (Kavanaugh & Dowd, 2004). The activity of histatin-5 is affected by the metabolic activity of candida, and activity is completely inhibited in the presence of respiratory inhibitors (Akkam 2013). Mitochondrial function and respiration are essential for histatin activity to occur, and non-respiring cells are resistant (Kavanaugh & Dowd, 2004).

The development of histatin-5 synthetically derived peptides with amino acid substitutions have increased stability and activity. Various histatin-5 synthetically derived peptides have been created in attempts to increase effectiveness and decrease the cost of production.

1.2.6 KM29

KM motif (Y-K-R-K-F) has been identified in histatin-5 for increased fungicidal activity. The creation of a peptide with increased effectiveness caused the creation of an inverted duplication of the KM motif, creating KM29. KM29 (Y-K-R-K-F-K-R-K-Y) is Histatin-5-derived antimicrobial peptide with high antifungal activity. It is 9 amino acid residues in length, cationic, and a symmetrical palindrome with equal activity in either direction. KM29 is not known to elicit an immune response (Kumar T. et al. 2011) and yields a fungicidal activity ten times greater than Histatin 5. KM29 is active against a variety of Candida species (Bullock et al. 2020), with minimal red blood cell hemolysis. Due to the efficient cost of production and no known negative effects, KM29 is a great antifungal agent that requires more analysis.

KM29 has been found to localize in the mitochondria for *S. cerevisiae* and *C. albicans* (Bullock et al. 2020) and it depends on the electron transport chain (ETC). Any mutation in the mitochondria, or respiration specifically, has rendered KM29 ineffective (Bullock et al. 2020). KM29 has been found to induce reactive oxygen species (ROS) production in *S. cerevisiae* and *C. albicans,* which was strongly linked with cell death (Bullock et al. 2020). Mitochondrial fragmentation has been associated with KM29 localization as well as mitochondrial membrane potential depolarization in *S. cerevisiae* (Bullock et al. 2020). This could be due to the electrostatic forces between the positive KM29 with the negative phospholipids on the mitochondria membrane.

KM29 has shown a high level of effectiveness in *saccharomyces* and *candida* species. It has been found when *S. cerevisiae* is grown under conditions that induce respiratory metabolism, such as lactate, the cells became more sensitive to KM29 (Akkam 2013).

1.3 CRISPR

The increasing effectiveness of CRISPR (clustered regularly interspaced short palindromic repeats) technology has made genome manipulation in a wide variety of organisms very accessible (Vyas et al. 2018). CRISPR genome editing usually only requires an RNA-guided

endonuclease, usually Cas-9, and guide RNA (gRNA) complementary to the targeted gene of interest (Raschmanová et al 2018). Using a solo vector CRISPR system (gRNA + Cas9) (Figure A), fewer selectable markers are required and provides a CEN/ARS element for plasmid maintenance along with ura3 marker (Vyas et al. 2018) was found to be beneficial in *S. cerevisiae, C. albicans,* and *N. castillii*. *C. glabrata* mutation rates were affected in the presence or absence of a repair template but preferred a CaCas-9 promoter (Vyas et al. 2018).

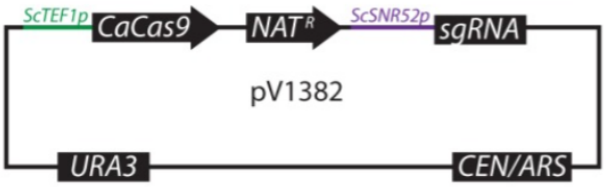

Figure B: Adapted from Vyas, V. K., Bushkin, G. G., Bernstein, D. A., Getz, M. A., Sewastianik, M., Barrasa, M. I., Bartel, D. P., & Fink, G. R. (2018). New CRISPR Mutagenesis Strategies Reveal Variation in Repair Mechanisms among Fungi. *mSphere*, *3*(2). https://doi.org/10.1128/msphere.00154-18

Cas9 was the first RNA-guided endonuclease reported and remains the most effective method to this day (Raschmanová et al 2018). Cas9 functions by using the guide RNA to locate the complementary sequence on the DNA, which is followed by a recognized protospacer adjacent motif (PAM) sequence, then creates a precise double--stranded cut (Vyas et al. 2018, Raschmanová et al 2018, Naito et al. 2014). PAM sites are not rare in a motif but are the limiting factor to achieve genomic precision (Labun et al. 2019).

The guide RNA is ~20 nucleotides in length and is followed by the PAM sequence which is 3 nucleotides long. It is important to ensure proper alignment to the target sequence as misalignment to avoid off-target editing (Naito et al. 2014). The double-strand break is repaired by one of two methods as observed in Figure C.. First, is non-homologous end joining (NHEJ), which often adds or removes bases resulting in insertions or deletions (indels) (Vyas et al. 2018). The second method, homology-directed repair (HDR), is much more precise and has fewer

unwanted genomic changes; however, it requires a repair template from the homologous chromosome or provided RNA sequence (Vyas et al. 2018). Increased efficiency in transformation in C. glabrata was found with the presence of a repair template; without, mutants acquire small insertions or deletions like the NHEJ repair (Vyas et al. 2018).

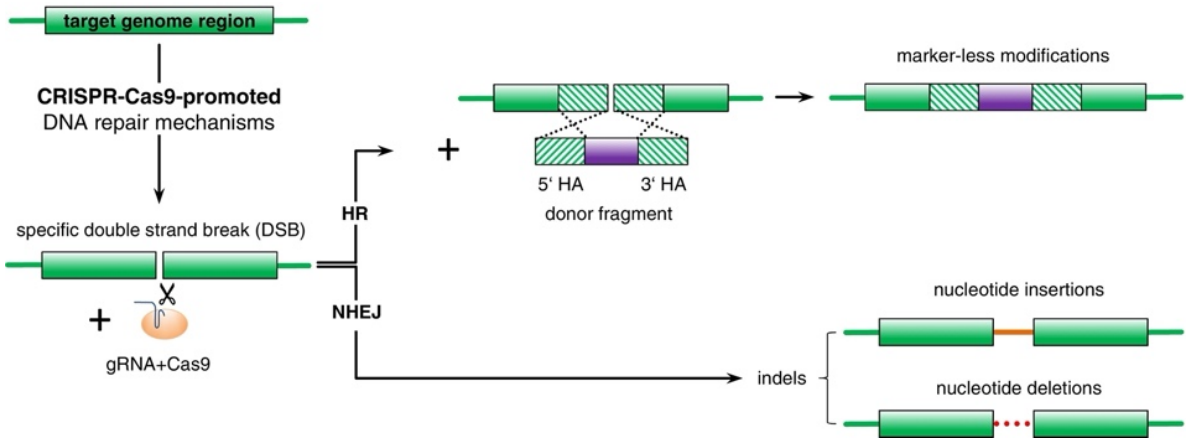

Figure C: Genetic modifications via CRISPR-Cas-promoted DNA repair mechanisms. Adapted from Raschmanová, H., Weninger, A., Glieder, A., Kovar, K., & Vogl, T. (2018). Implementing CRISPR-Cas technologies in conventional and non-conventional yeasts: Current state and future prospects. *Biotechnology Advances*, *36*(3), 641–665. https://doi.org/10.1016/j.biotechadv.2018.01.006.

1.6 Targeted Genes:

A genomic screen of deletions in *S. cerevisiae* that demonstrated increased resistance to KM29 based on a modified minimal inhibitory concentration (MIC) assay that was used for screening (Sites 2018). Of the ~4,800 non-essential deletion in the screen, 27% demonstrated increased resistance to KM29. The leading group with changes in cellular process was mitochondrial function, with the second largest group being plasma membrane transport (Sites 2018). Membrane transport genes were tested in a killing assay with KM29 to determine the significance of resistance. A few of the membrane transport genes that demonstrated increased resistance in *S. cerevisiae* included groups of metal transport (*FET4, ZRT2*), hexose transport (*HXT2, HXT3, HXT5, HXT10*), polyamine transport (*AGP2* & *SKY1*), and sterol transport (*LAM1*

& SIP3). Genes of significant increased resistance in *S. Cerevisiae* were used for deletion in *C. glabrata*; then tested against increased concentrations of KM29.

Hexose transport is critical to cell survival as it regulates cell metabolism by providing essential elements. It is found that hexose transporters (*HXT1, HXT2, HXT3, HXT13*) function by maintaining a steep influx-directed D-glucose gradient (Aouida et al. 2005) with either a high or low affinity. Glucose can undergo respiration or fermentation to release energy for the cell. Respiration occurs in the mitochondria and produces a lot more-ATP-compared to fermentation, which takes place in the cytoplasm and produces very few ATP molecules. With the importance of glucose for numerous cellular processes and its breakdown that occurs in the mitochondria, observing the effects of antifungal transportation through this hexose transport is intriguing.

Metal transport is essential for protein folding, cell growth, gene transcription, and respiration. It has been found that Zn^{2+} plays a role in increasing the effectiveness of histatin-5 against candida species (Norris et al. 2020). By observing the effect of metal transport genes against a histatin-5 derived antifungal, it will provide a better understanding of the function against antifungals.

Polyamine transport is regulated polyamine homeostasis in a cell, which is essential for its growth and proliferation. *AGP2* is thought to have a role in positive regulation of (R)-carnitine transmembrane transport and positive regulation of polyamine transmembrane transport (CGD) in Candida species. It has been found that in *S. cerevisiae*, *AGP2* is a member of the YAT family, which is a major component of membrane transport. Agp2p permease has reported a high affinity for polyamine import and can act via 1 of three proposed mechanisms: -1) a dual specificity for carnitine and polyamine transporter, 2) a plasma membrane sensor, or 3) a mixed permease and sensor model (A, B, C: Aouida et al. 2005).

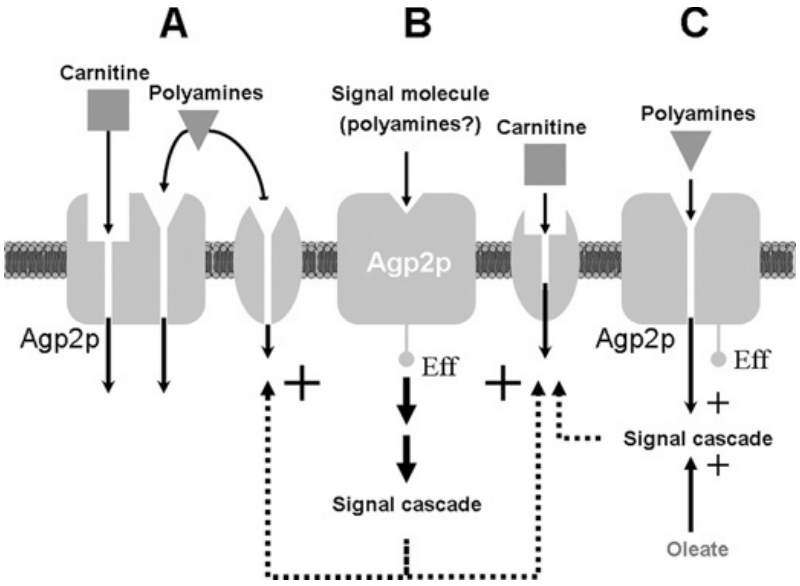

Figure D: Adapted from Aouida, M., Leduc, A., Poulin, R., & Ramotar, D. (2005). AGP2 Encodes the Major Permease for High Affinity Polyamine Import in Saccharomyces cerevisiae. *Journal of Biological Chemistry*, *280*(25), 24267–24276. https://doi.org/10.1074/jbc.m503071200

There are three polyamines, spermidine, spermine, and putrescine that are essential organic cations which regulate a variety of cellular processes. A few of those processes include nucleic acid and protein synthesis, and cell growth (Kumar R. et al. 2011), post-translational modification eIF-5A, and gating of several ion channels (Aouida et al. 2005). Polyamines are found to preferentially bind GC-rich regions of genomic data, acting as a repressor of transcription (Igarashi & Kashiwagi, 2000). The plasma membrane is responsible for the movement of polyamines and by targeting a polyamine transporter we should be able to validate *AGP2* function as a polyamine transporter.

AGP2 is reported to have a high affinity for spermidine (and polyamines) and found to localizes to the plasma membrane (Aouida et al. 2005). In *S. cerevisiae* the deletion of *AGP2* decreases spermine and spermidine uptake, representing a strong resistance against toxicity of polyamines (Aouida et al. 2005). *AGP2* negatively regulates three classes of genes in *S. cerevisiae* involved in "(i) lipid/fatty acids oxidation and mitochondrial oxidative metabolism

(Krebs cycle and respiration) (ii) plasma and peroxisomal membrane transport and (iii) meiosis and sexual spore formation" (Aouida et al. 2005). *SKY1, ZRT 2, HXT2,* and *HXT3* have been downregulated because of *AGP2* deletion in *S. cerevisiae* (Aouida et al. 2005). Due to *AGP2* function as a membrane sensor, the downstream gene *SKY1* is of importance, and has been found to regulate polyamines. *SKY1* is known to be an SRPK1-like protein kinase involved in mRNA splicing on the 3' end, involved in phosphorylation, and modulates cation uptake and homeostasis through membrane transporters (SGD). *SKY1* has also been demonstrated to be involved in osmotic stress and polyamine resistance in *C. glabrata* (CGD). KM29 could be channeled through the cell by *AGP2* or *SKY1* due to the affinity for cations making polyamine transporters interesting to investigate.

LAM members are known as **l**ipid transfer protein **a**nchored at a **m**embrane contact site, which plays a role in sterol transport (Gatta et al. 2015). *LAM1* has a paralog, *SIP3*, which both utilize StART-like domains (Gatta et al. 2015). They are one of six StART-like domain-containing proteins in yeast that may be involved in sterol transfer between the endoplasmic reticulum (ER) and the plasma membrane (PM) (SGD). It has been found that in the absence of either or both *LAM1* and *SIP3* reduces the rate of which exogeneous sterols are trafficked from the plasma membrane to the endoplasmic reticulum (Gatta et al. 2015). The deletion of a sterol transport has been associated with increased resistance to amphotericin B (Gatta et al. 2015). The mechanism of action to transport sterol between the ER and PM is unknown and requires further investigation (Gatta et al. 2015).

The need to identify a novel target gene in *C. glabrata* is necessary to understand the functions and relation to other yeast species. Due to *C. glabrata's* increased resistance to antifungals, the cause of life-threatening conditions with limited treatment options makes understanding this species of utmost importance. The present study used *S. cerevisiae* as a guide for targeting transporter genes for validation to then understand the mechanism of KM29 in *C. glabrata*. The genome-wide screen in *S. cerevisiae* deletions treated with KM29 through gene

ontology determined four of the seven processes affected are related to mitochondrial genes, through an increased sensitivity to KM29. This served as a guide to complete a CRISPR-Cas9 deletion of the gene of interest in *C. glabrata* which was validated by the completion of a killing assay with KM29.

CRISPR Cas-9 deletions constructed in *C. glabrata* were created using vectors from Vyas et al. 2018 that have been designed with high efficiency for *C. glabrata*. Due to *C. glabrata's* preference to complete non-homologous repair the presence of a repair template was required to direct C. glabrata to complete homology-directed repair for increased transformation effectiveness. The web program CHOPCHOP was used to create gRNAs in this study with minimal off-site binding.

MATERIALS AND METHODS

Yeast strains

All *Saccharomyces cerevisiae* strains used in this study were derivatives of BY4741 (*MATa his3*Δ1 *leu2*Δ0 *met15*Δ0 *ura3*Δ0) (Brachmann et al. 1998), the parent strain of the whole genome deletion library used for the genetic screen that identified the gene candidates characterized in this work (Bullock et al. 2020). Strains carrying gene deletions were obtained from this deletion library.

Candida glabrata NCCLS 84 (ATCC 90030) or CBS 138 (ATCC 2001) were used for the construction of deletion mutants and further characterization. All yeast strains were grown on standard YPD medium (1% yeast extract, 2% peptone, 2% glucose) at 30° C, unless indicated. Solid media contained 2% agar (Difco). Selective plates for kanamycin resistance in yeast contained YPD with 200 µg/ml of G418 (SIGMA), or YPD with 100 µg/ml ClonNat (Werner) for nourseothricin resistance.

Generation of double mutant *lam1*Δ *sip*3Δ in *S. cerevisiae*

The *lam1*Δ::KanMX4 *sip*3Δ::KanMX4 was obtained by first crossing *sip3*Δ::KanMX4 from the deletion collection (*MATa sip3*Δ::KanMX4 *his3*Δ1 *leu2*Δ0 *met15*Δ0 *ura3*Δ0) with AWx1-3A (*MATα trp1*Δ63, *lys2*Δ202, *ura3*$^{-)}$ to obtain a *MATα sip3*Δ::KanMX4 derivative. The resulting diploid was sporulated in 1% potassium acetate, ascospores dissected and segregants were screened for all the parental markers. This new strain was then crossed to the *lam1*Δ::KanMX4 from the deletion collection (*MATa lam1*Δ::KanMX4 *his3*Δ1 *leu2*Δ0 *met15*Δ0 *ura3*Δ0). The diploid was sporulated and ascospores were dissected. Double mutants containing *lam1*Δ::KanMX4 *sip*3Δ::KanMx4 were identified in non-parental ditype (NPD) tetrads.

Fungicidal activity of KM29 against *S. cerevisiae* and *C. glabrata*

The fungicidal activity of KM29 was tested using microdilution plate assays as indicated (Bullock et al. 2020). Briefly, individual yeast colonies were resuspended in 5 mM sodium phosphate buffer (NaP), cells were counted and adjusted to a cell density of $1.5x10^5$ cells/ml. Cells were incubated with various concentrations of KM29 (1, 2.5, and 5 μM for *S. cerevisiae* and 5, 10, and 20 μM for *C. glabrata*) in a shaking incubator at 220 rpm for 2 hours at 30°C and plated on YPD. Colony forming units (CFUs) were counted after 48 h and percent survival was calculated as $\frac{colonies\ from\ suspension\ with\ peptide}{colonies\ from\ suspension\ without\ peptide} X100$. Biological replicas from individual colonies were conducted a minimum of three times for each experiment.

Statical Analysis

A minimum of three biological replicates were included in all calculations. Error bars represent the standard error of the mean. Two-way ANOVA was used for multiple comparisons. Data were analyzed and plotted using GraphPad Prism. Statistically significant differences from

the wild-type strain are indicated by asterisks above bars (*, $P < 0.05$; **, $P < 0.01$; ***, $P < 0.001$).

CRISPR Cas9 for AGP2 and LAM1 deletion in *C. glabrata*

Construction of the guide RNA (gRNA) was done as described (Vyas et al. 2018) The selection of the target DNA immediately upstream of a 3 base-pair PAM (protospacer adjacent motif) site was determined using the CHOPCHOP web program (https://chopchop.cbu.uib.no/). Primers were created based on location of the target gene, a GC content of 40-60%, and a low score and minimal offsite binding when completing a BLAST against the entire genome in *C. glabrata* database (candidagenome.org). All primers were synthesized by Eurofins Genomics. The plasmid vector pV1382 (Vyas et al. 2018) containing the Cas9 gene was used to clone the gRNA using the BsmBI restriction site as follows. Phosphorylation of the primers was done by combining 6.5 µL of sterile H_2O, 1 µL forward gRNA primer, 1 µL of reverse gRNA primer, 1 µL of 10x T4 ligation buffer with 10 mM ATP (NEB), 0.5 µL of T4 polynucleotide kinase (NEB) in a PCR tube. The phosphorylation and annealing reactions were done by incubating the tube in a thermocycler at it for 30 min at 37°C, followed by 5 min at 95°C, followed by a ramp down to 20º at 5ºC/min. The annealed gRNA was ligated to the pV1382 vector digested with BsmBI following the manufacture's instruction (NEB). Prior to ligation, the vector was dephosphorylated by adding 1 µL of QuickCIP (NEB) to the 20 µL digestion reaction, incubating at 37ºC for 10 min, then transfer to 80ºC for 20 min. The ligation reaction was set up by combining 4 µL of sterile H_2O, 10 µL quick ligase 2x reaction buffer, 3 µL of digested and dephosphorylated vector, 2 µL of a 1:200 dilution of annealed gRNA insert and 1 µL of QuickLigase (NEB). The reaction was incubated in a 25ºC water bath for 5 min. The control ligation of vector with no insert omitted the insert, replacing it with 2 µL of water.

The ligation reaction was used to transform *E. coli* (either NEB 5- α , NOVA Blue or XL1 blue strains) following standard procedures. Transformation reactions were plated on LB + ampicillin plates and incubated overnight at 37ºC. Plasmid DNA was isolated from 6 positive colonies (vector + insert) using a QiaPrep Spin mini prep kit (Qiagen). Plasmid DNA was sequenced (SimpleSeq, Eurofins Genomics) using a primer that annealed upstream of the BsmBI insertion site in pV1382. Correct plasmids were saved for transformation of *C. glabrata.*

A repair template was used to facilitate homologous recombination to create a deletion that extended to the natural stion codon of the target gene (*AGP2*). Two 60 bp long primers with last 10 bp at their 3' end overlapping, were used to amplify the DNA using PCR. In a 50 µL reaction, 0.5 µL of the forward and reverse primers were combined with 37 µL H_2O, 10 µL of 5 x buffer, 1 µL of dNTP's, 0.5 µL $MgCl_2$ and 0.5 µL Phusion polymerase (Thermo Fisher). The PCR was set up for 30 cycles as follows: 98ºC for 30 sec, 98ºC for 10 sec, 56.8ºC for 30 sec, 72ºC for 30 seconds, and a final extension at 72ºC for 5 min. 5 µL of PCR product was analyzed on a 1% agarose gel and the remaining was purified using a QiaQuick PCR purification kit (Qiagen) and eluted in 30 µL of deionized water at pH 7.8.

C. glabrata transformation was done following Vyas et al. (2018). Cells from an overnight culture were harvested, washed with TE/LiOAc buffer (10 mM TRIS 1 mM EDTA pH 8.0) and resuspended in 2 ml of TE/LiOAc buffer with 25 mM DTT. The cell mixture was incubated in a roller drum at 30ºC for 15 h. followed by two washes with 5 ml of ice-cold water, one wash with 5 ml of ice-cold 1 M sorbitol and resuspended in 500 µL of ice-cold 1 M sorbitol. 40 µL of the chilled cell suspension was mixed with 0.3 ug of plasmid DNA and added to a chilled Bio-Rad Gene Pulser cuvette. Electroporation was conducted on a Invitrogen Gene pulser with a capacitance of 25 uF, resistance of 200Ω at 1.8kV. 100 µL of YPD was immediately

added to the cuvette and incubated 1 h at room temperature. The mix was plated on selective medium (YPD + nourseothricin) and incubated at 30º for two days. Yeast colonies were screened for the deletion by PCR using primers flanking the Cas9 target and repair template genomic region. Positive candidates by PCR were further confirmed by DNA sequencing of the PCR product (Eurofins Genomics). Primers used for PCR are indicated in Tables 1 and 2.

Table 1: *C. glabrata AGP2* Gene Deletion guide RNA and repair template

Location		**Strand**	**Sequence**
Upstream	gRNA	Forward	5' GATCGTAGAGAGCACCAGCACACACG -3'
Downstream	gRNA	Reverse	5' AAAACGTGTGTGCTGGTGCTCTCTAC -3'
Upstream	Repair template	Forward	5'ATCTCTTTTGACGAAGACGAGAGGAGCAGTAAT GACTCGAGGACTCAGCTGATAAAATTA -3'
Downstream	Repair template	Reverse	5' TTAAAATAAAAATTTGGTGCCGAGTAATTTACA ATGTAAATAATTTTATCAGCTGAGTCC -3'

Table 2: *AGP2* Sequencing and Amplification Primers

Location	**Location**	**Strand**	**Sequence**	**Species**
Upstream	Cut site	Forward	5'CTAGCGGTAAAGGTGCGCAT 3'	PV1382
Upstream 100bp	gRNA	Forward	5'GATGACAAGTTCCCATCGGTTA 3'	C. Glabrata
Downstream	100 bp after stop	Reverse	5'GATAGCTGCTTTTAAGAATACCA 3'	C. Glabrata
Upstream	ATG Start	Forward	5'ATGGTGAGTTGCTTGTGTTGC 3'	C. Glabrata
Downstream	200 bp after stop	Reverse	5'GTGCCACTCTTCTACCAACTA 3'	C. Glabrata
Upstream	420 bp before gRNA	Forward	5'CTTCGTGAAGTAGACTGCCA 3'	C. Glabrata

Phenotypic analysis of *S. cerevisiae* and *C. glabrata* deletion strains

Phenotypic characterization of *agp2*Δ mutants in *S. cerevisiae* and *C. glabrata* was carried out by serial dilution and spotting on various media associated with distinctive phenotypes in *Candida* species. For serial dilutions, 1 ml of an overnight culture on YPD was adjusted to 1 x10^7 cells/ml and four 10-fold dilutions were done with sterile water before plating 4 µl on various media.

For disk diffusion assays used to test sensitivity to polyamines, 5 mm sterile filter paper disks were placed on a loan of fungal cells plated on YPD and 5 µl of water, 344 mM spermine (SPM), 247 mM spermidine (SPD), or 620 mM putrescine (PUT) was applied to each filter. Plates were incubated at 30°C and 37°C for one day. The growth inhibition was measured in mm across the diameter of the disc, extended to the edges of zone clearance.

Growth curves of *C. glabrata agp2*Δ mutants

Wild type *C. glabrata* and three confirmed *agp2*Δ mutants were grown overnight on YPD. A 1:1000 dilution (100 µl of the overnight culture in 100 ml of YPD) was incubated at 30°C with shaking and 1 ml samples were taken every 2 hours to measure their optical density (OD_{600}) using YPD as blank in a Beckman DU 530 Life Science UV/Vis Spectrophotometer.

RESULTS

Validation of *S. cerevisiae* mutants isolated in the screen for increased resistance to KM29.

In previous work, the sensitivity *C. glabrata* to KM29 was used to screen the whole genome deletion library for genes that when deleted caused increased sensitivity to the peptide, aiming at identifying genetic pathways involved in the killing mechanism used by KM29

(Bullock et al). In addition to the clear involvement of respiratory genes and mitochondrial function, many other pathways were identified, including several kinds of transporters. Among these were various hexose transporters and metal transporters. First, we conducted a validation analysis of the increased resistance to the fungicidal activity of KM29 by mutants in the four hexose transporters identified in the screen (*HXT2*, *HXT3*, *HXT5*, and *HXT10*) using a microdilution assay. The data shown in Figure 1 indicates an increase in resistance in the *hxt3*Δ strain treated with 2.5 and 5 μM KM29, but very little or no effect in the survival of *hxt2*Δ*,* *hxt5*Δ*,* and *hxt10*Δ strains in any of the KM29 dosages assayed. Considering the redundancy and structural conservation of hexose transporters in *S. cerevisiae* (7 functional *HXT* genes) and the equivalent number of orthologs in *C. glabrata*, along with the minimal effect seen in *S. cerevisiae* for 3 of the 4 mutants tested, we decided not to proceed with the study of these transporters in *C. glabrata*.

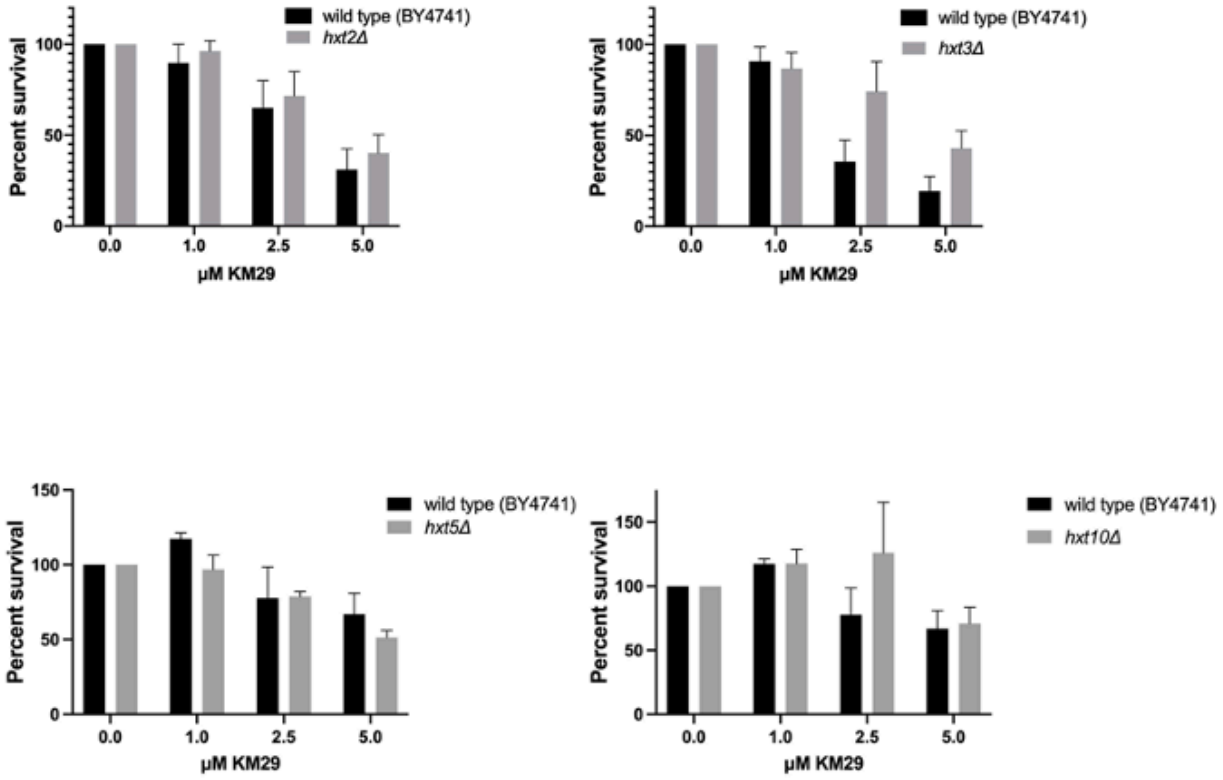

Figure 1. *Saccharomyces cerevisiae* hexose transporter deletion. The *hxt*Δ mutants do not demonstrate significant resistance to the fungicidal activity of KM29 peptide in comparison to the wild-type strain.

We next tested the fungicidal activity of KM29 against *S. cerevisiae* mutants in two metal transporters, *FET4* and *ZRT2*. Fet4 is a low affinity iron permease, and Zrt2 is a low affinity zinc transporter. The survival data from *fet4*Δ and *zrt2*Δ strains compared to wild type is shown in Figure 2. The deletion of *FET4* did not show any significant change in the susceptibility to KM29 at any concentration of the antifungal. Similarly, the deletion of *ZRT2* did not show increased resistance to KM29 when compared to wild type levels. Although there was a tendency to increased survival values in *zrt2*Δ at all concentrations of the peptide, those differences where not statistically significant and therefore these metal transporter genes were not analyzed further.

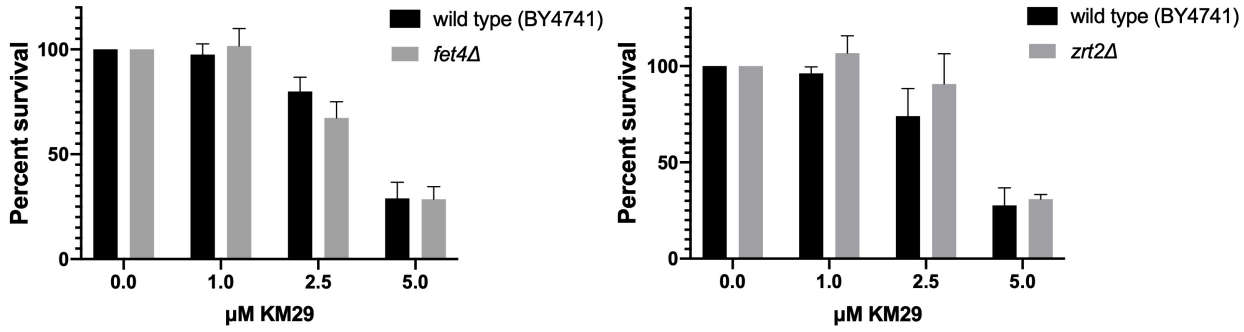

Figure 2: *Saccharomyces cerevisiae* metal transporter deletion. The *fet4*Δ mutant and zert2Δ do not demonstrate significant resistance to the fungicidal activity of KM29 peptide in comparison to the wild-type strain.

In *S. cerevisiae*, *AGP2* is a plasma membrane protein involved in the regulation of polyamine and carnitine transport. The increased resistance associated with *agp2*Δ in the yeast deletion screen was interesting because it has been shown that histatin 5 can have increased fungicidal activity against *C. glabrata* when the fungal cells overexpress a *C. albicans* polyamine transporter (Tati et al. 2013). Therefore, we set out to validate the KM29 resistance in *S. cerevisiae agp2*Δ. As illustrated in Figure 3, the deletion *agp2*Δ led to significant cell survival at 2.5 and 5 μM KM29. Since *AGP2* has been shown to regulate the expression of the Sky1, a SR kinase which also plays a role in polyamine transport (Aouida et al 2005), we examined the fungicidal activity of KM29 against a *sky1*Δ strain. Figure 4 shows increased resistance of *sky1*Δ cells to KM29 at 2.5 and 5 μM concentrations, consistent with the survival values obtained for *agp2*Δ strains. We concluded that *AGP2* was a good candidate gene for deletion and characterization in *C. glabrata.*

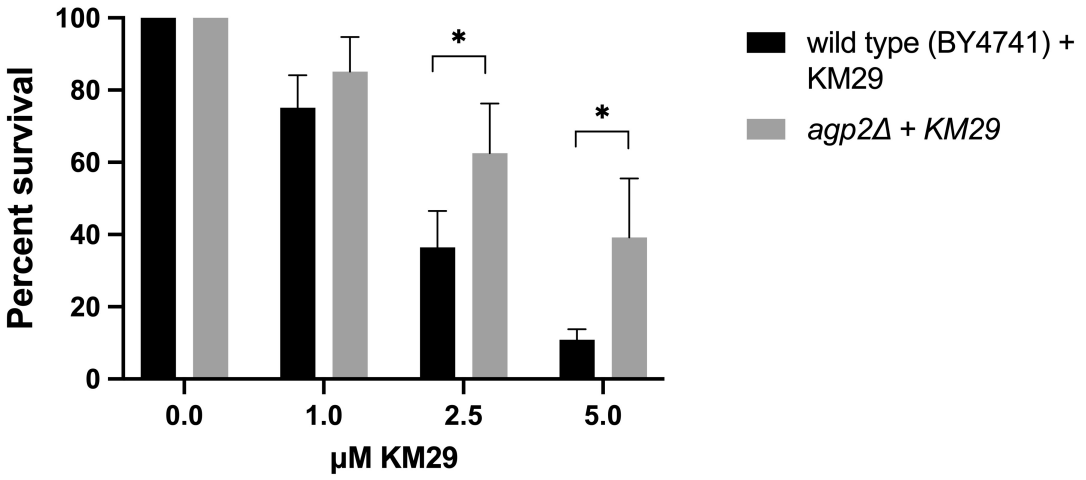

Figure 3: *Saccharomyces cerevisiae* polyamine transporter deletion. The *agp2*Δ mutant demonstrates significant increase in resistance to the fungicidal activity of KM29 peptide in comparison to the wild-type strain.

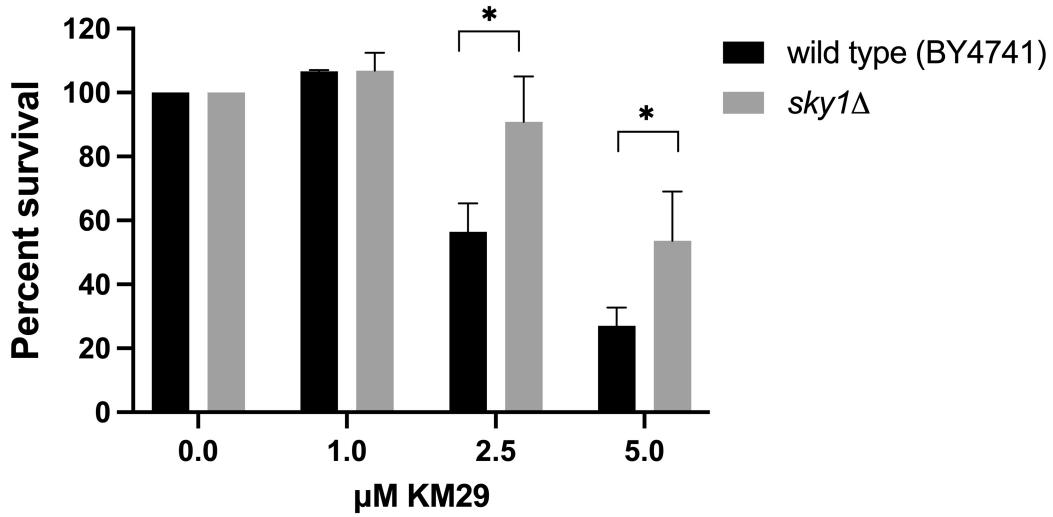

Figure 4*: Saccharomyces cerevisiae* SR protein kinase deletion. The *sky1*Δ mutant demonstrates significant increase in resistance to the fungicidal activity of KM29 peptide in comparison to the wild-type strain.

LAM1 and *SIP3* are paralogs in *S. cerevisiae* with homologous counterparts in the *C. glabrata* genome. Deletions of both genes were identified in the genetic screen in *S. cerevisiae* for increased resistance to KM29. *LAM1* belongs to the *LAM* family of genes named for their **l**ipid transfer protein **a**nchored at a **m**embrane contact site, that play a role in sterol transport. Although their function has not been fully elucidated, both genes encode proteins that contain a StART-like domain which binds lipids and may be involved in sterol transfer between intracellular membranes (Gatta et al. 2015). Disruption of their function results in an increase in plasma membrane sterol content, potentially affecting the uptake of KM29. Thus, we tested the killing activity of KM29 against *lam1*Δ and *sip3*Δ strains (Figure 5). The deletion of *LAM1* in *S. cerevisiae* resulted in significant cell survival to KM29 at 2.5 and 5 μM concentrations and the deletion of *SIP3* caused significant resistant to the peptide at 2.5 μM concentration. Considering the limited information about the function of Lam1 and Sip3, but likely having the same or similar role in sterol transport, we decided to build a *lam1*Δ *sip3*Δ double mutant strain and test its susceptibility to KM29 killing. Starting with the individual mutants from the deletion collection, genetic crosses were carried out to obtain a double deletion *lam1*Δ::KanMX4 *sip*3Δ::KanMX4 strain as indicated in the Methods section. Figure 5 shows the data for KM29 killing activity, indicating that the *lam1*Δ *sip*3Δ mutant was significantly more resistant to KM29 at 2.5 and 5 μM concentrations than the wild-type strain, but it did not show any additive effect. We concluded that these results warranted exploring the effect of the *C. glabrata LAM1* homolog deletion (and *SIP3* depending on the results) with respect to KM29 susceptibility.

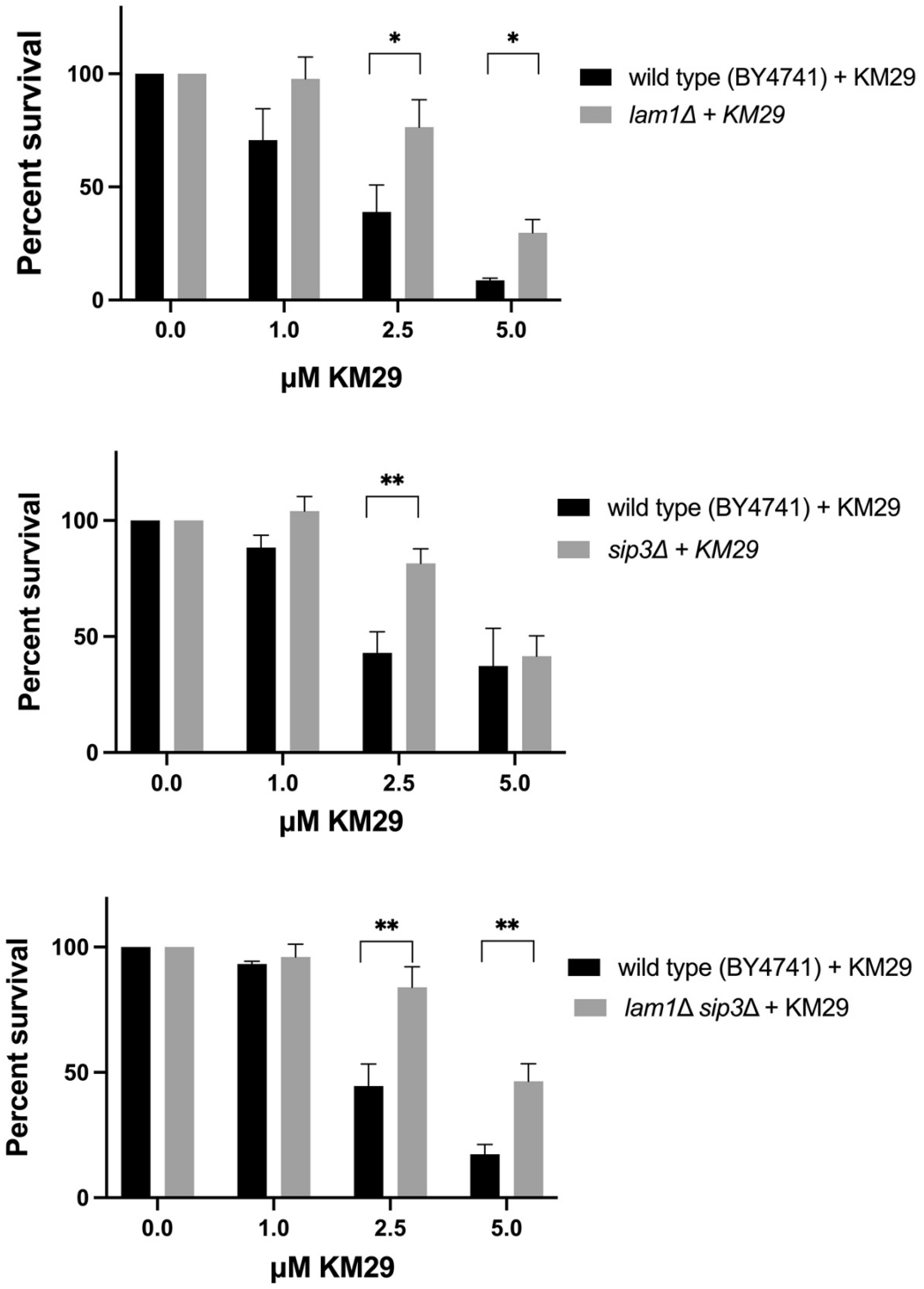

Figure 5: *Saccharomyces cerevisiae* sterol transporter deletion. The *lam1*Δ mutant and *sip3*Δ mutant independently demonstrate significant increase in resistance to the fungicidal activity of KM29 peptide in comparison to the wild-type strain. The double mutant *lam1*Δ*sip3*Δ demonstrate significant increase in resistance to the fungicidal activity of KM29 peptide in comparison to the wild-type strain.

Deletion of *C. glabrata AGP2* gene.

The set up for deletion of *C. glabrata AGP2* using CRISPR-Cas9 involved the selection of the vector to be used for the construction of the guide RNA, design of the primers for the guide RNA and cloning the PCR product into the vector. Once the guide RNA plasmid was verified by DNA sequencing it was used to transform *C. glabrata*, along with a repair template. *C. glabrata* uses preferentially non-homologous end joining to repair double strand breaks, therefore it is necessary to add a repair template to direct homologous recombination to the desired deletion provided in the template (Vyas et al 2018). The plasmid pV1382 was used to build the guide RNA to target Cas9 to the *AGP2* locus. We performed yeast transformations with and without repair template, to compare the effectiveness of both types of repair processes, and selected for resistance to nourseothricin, the selectable drug cassette in pV1382. Figure 6 shows the clear increase in colonies present on the plate that included the repair template, compared with the one that only contained the pV1382 plasmid. Several colonies were isolated, streaked for single colonies and tested for the deletion of *AGP2* by colony PCR. Figure 7 shows an example of the PCR products obtained, where the deletion the smaller bands represent *agp*2Δ constructs. To verify these constructs as having the correct deletion, genomic DNA was purified, a longer PCR was generated and sent out for DNA sequencing with primers annealing upstream and downstream of the deleted region. Three correct strains were used for further characterization.

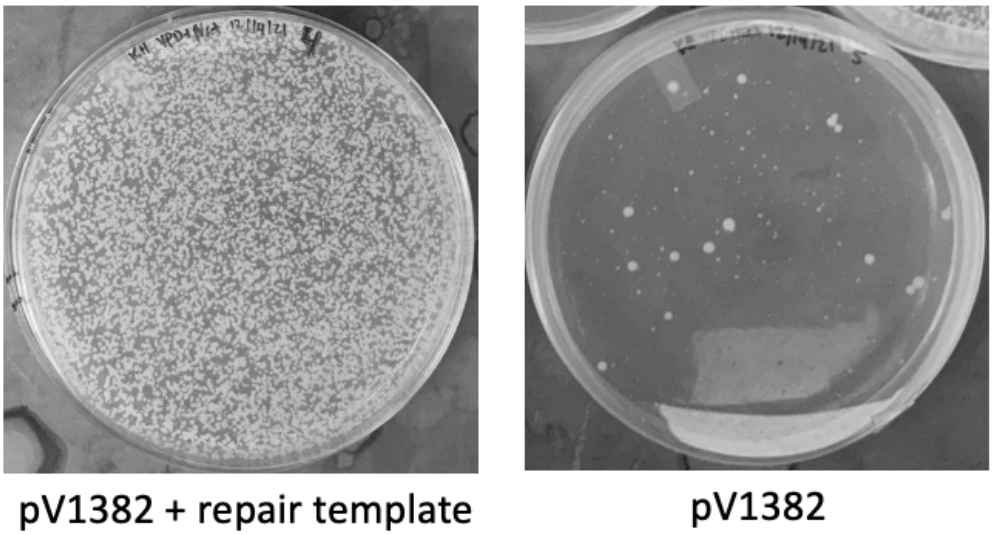

Figure 6: *C. glabrata agp2*Δ transformation results.

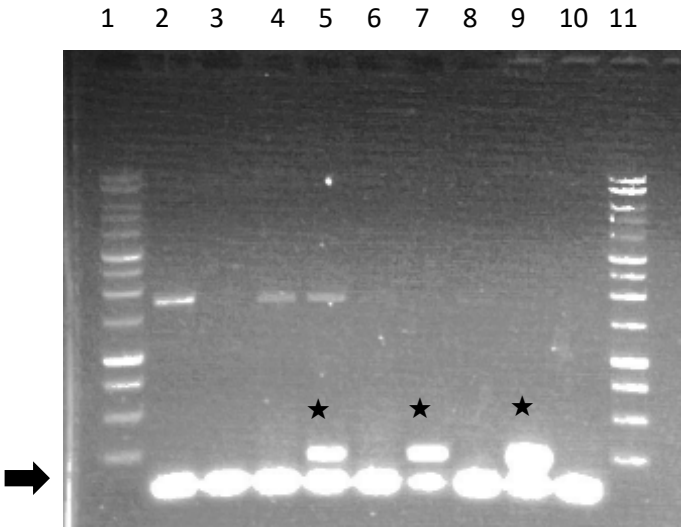

Figure 7: PCR Gel Electrophoresis. Lane 1: Promega 1 kb ladder. Lane 2: #13 Lane 3: #14. Lane 4: #15. Lane 5: #16. Lane 6: #17. Lane 7: #18. Lane 8: #19. Lane 9: #20. Lane 10: C. glabrata (wild type). Lane 11: Promega 1kb ladder. Black arrow (➔) indicates expected band size due to *agp2*Δ, as expressed in lanes 5, 7, and 9 indicated by black star (★).

Characterization of *C. glabrata agp*2Δ.

Our main interest was to test the effect of KM29 in a *C. glabrata agp*2Δ strain to determine whether the *S. cerevisiae* results showing increased resistance to KM29 could be extended to *C. glabrata*, and effectively use the results of the *S. cerevisiae* deletion screen as a starting point to understand the mechanism of action of KM29 in *C. glabrata*. Microdilution assays were used to test the fungicidal activity of various concentrations of KM29 against *C. glabrata* wild-type and *agp*2Δ strains. Three *agp*2Δ strains confirmed by DNA sequencing were assayed. As shown in Figure 8a, *agp*2Δ mutant 1 showed a limited, and not significant, increase in resistance to KM29. However, *agp*2Δ mutants 2 and 3 were similar in resistance. Their combined data is shown in Figure 8b, displaying increased resistant at 5 μM and 10 μM KM29. It is not clear why one of the *agp*2Δ strains showed no difference, although the other two did and correlated with the *agp*2Δ data from *S. cerevisiae*.

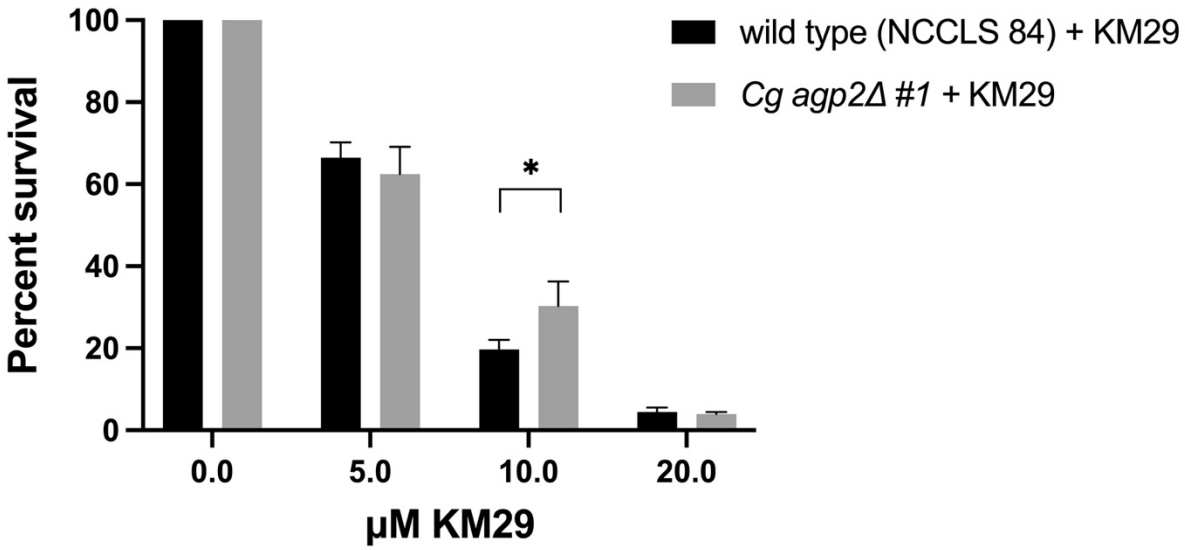

Fig 8a – *Candida glabrata* polyamine transporter deletion. #1*agp2*ΔCg mutant demonstrates light increased resistance to the fungicidal activity of KM29 peptide in comparison to the wild-type strain.

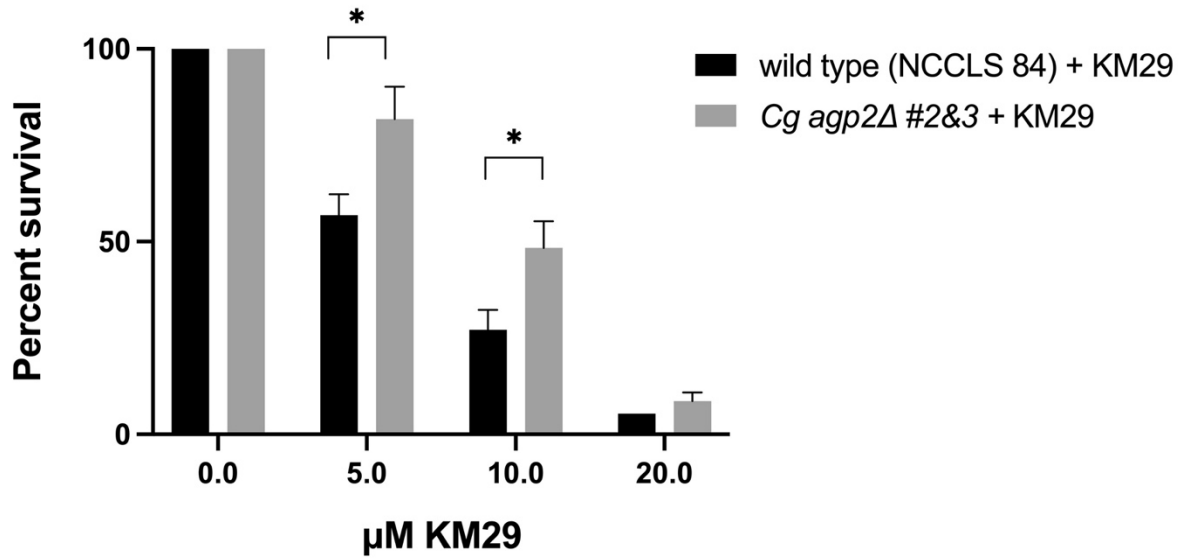

Fig 8b - Candida glabrata polyamine transporter deletion. #2 and #3agp2Δcg mutants demonstrate increased resistance resistance to the fungicidal activity of KM29 peptide in comparison to the wild-type strain.

To further characterize the *C. glabrata agp*2Δ mutants we tested sensitivity to three polyamines: spermine, spermidine, and putrescine. *S. cerevisiae agp*2Δ strains show resistance to spermidine and spermine toxicity (Aouida et al. 2005), therefore we asked whether polyamine sensitivity is affected in the *C. glabrata agp*2Δ mutants. Figure 9 shows a disk diffusion assay with various concentrations of the tested polyamines at 30°C and 37°C. No differences were observed between the wild type and any of the *C. glabrata agp*2Δ strains tested, although spermine showed a zone of inhibition at all the concentrations tested. We did not observe the expected resistance based on the published data for the *S. cerevisiae agp*2Δ strain either. To be consistent with the reported results, we used the same approach and tested growth of serial dilution of *S. cerevisiae* and *C.* glabrata *agp*2Δ strains along with the corresponding parental wild-type strains on YPD containing either 8 mM or 16 mM spermidine. As shown in Figure 10, no difference in growth was observed between *agp*2Δ and wild-type strains, therefore we cannot conclude that *agp*2Δ mutants are affected by exposure to polyamines under the conditions assayed.

1 – 5µL 247mM SPM 3 – 40 µL 247mM SPM

2 – 10 µL 247mM SPM 4 – 5 µL H_2O

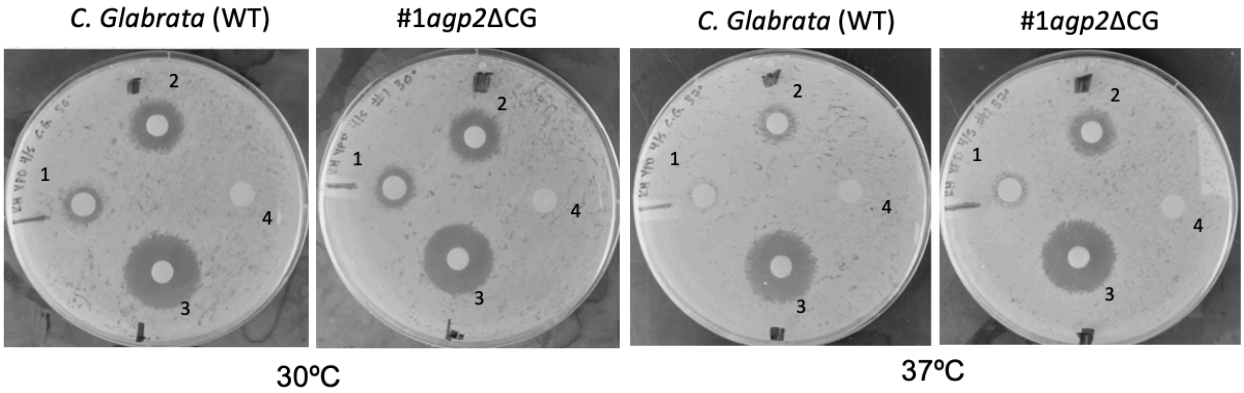

Figure 9- Susceptibility of *C. glabrata* strains to spermine. A) wild type *C. glabrata* compared to #1*agp*2Δcg with increasing concentrations of spermine at 30ºC and 37ºC. The growth rate between the two was the same, with slightly increased growth rate at 37ºC, but no differences on the growth around the disks between wild-type and #1*agp*2Δ strains.

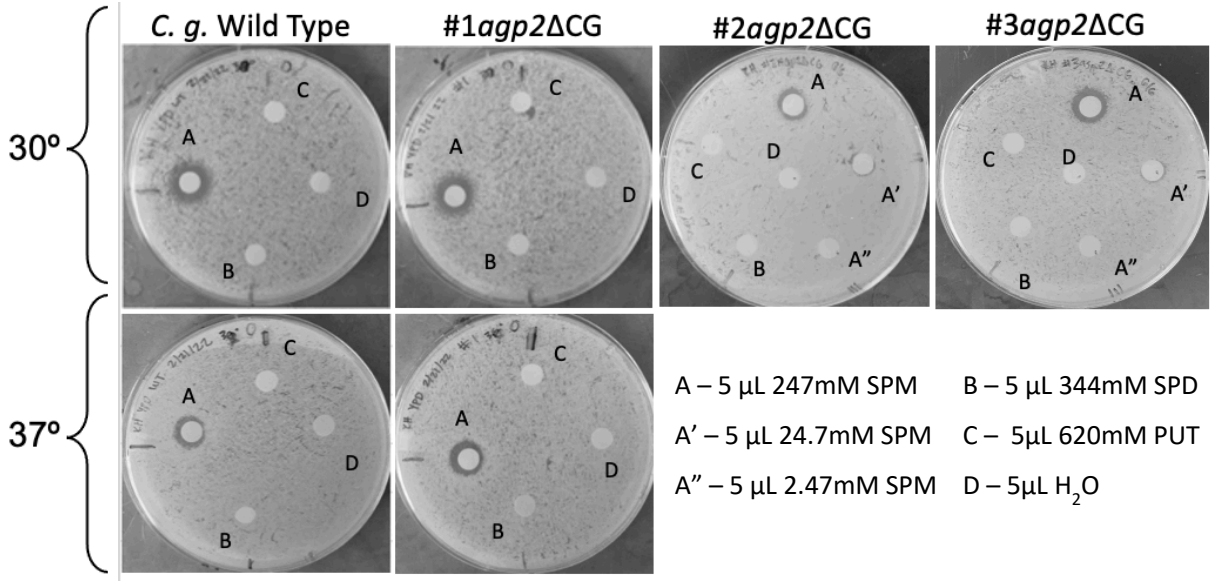

Figure 9 - B) Growth of *C. glabrata* and mutant against polyamines. Based on the growth around the disk assay, there is no noticeable difference in the growth of polyamine mutants #1,2,3 at either 30ºC or 37ºC when compared to the wildtype *C. glabrata.*

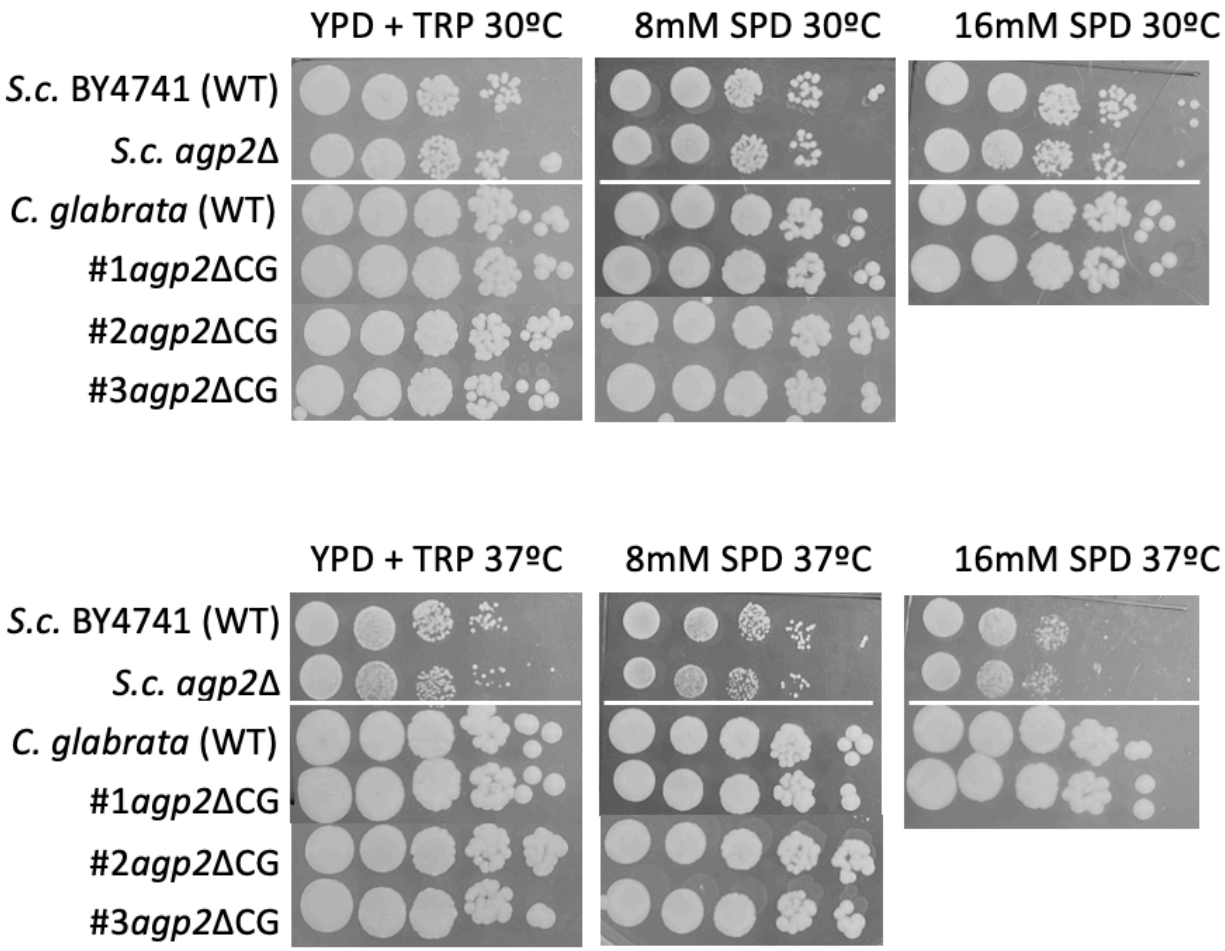

Figure 10 – *Saccharomyces cerevisiae* and *Candida glabrata* serial dilution on 8mM and 16 mM spermidine (SPD) medium. *S. cerevisiae* WT and *agp2*Δ demonstrate the same growth rate, with decreased growth rate at 37ºC. *C. glabrata* and polyamine mutants #1*agp2*Δcg, #2*agp2*Δcg, #3*agp2*Δcg do not demonstrate and difference in growth across the various temperature or concentration of spermidine.

To compare the rate of growth between the wild type *C. glabrata* and *agp2*Δ mutants, we measured the optimum density (OD_{600}) over 10 hours. We did not identify a significant different in growth rate between the samples as seen in Figure 11.

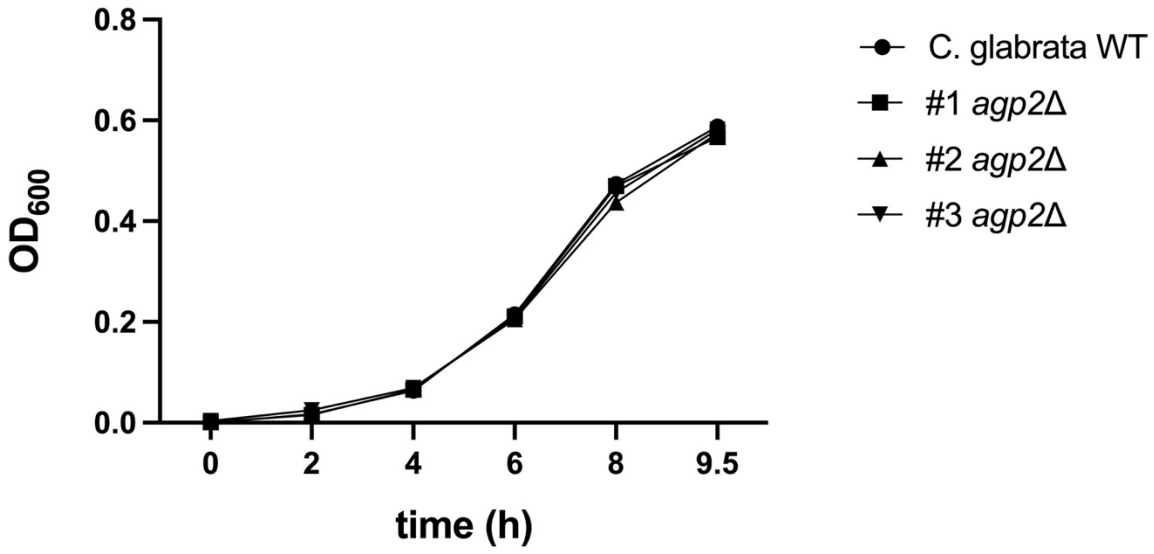

Figure 11: *Candida glabrata* growth curve. C. glabrata and *agp2*Δ transporter mutants demonstrate the similar rate of growth overtime with no significant differences.

To identify some phenotype associated with the *C. glabrata agp*2Δ mutant, we tested growth on a variety of media used to reveal growth or colony morphology differences associated with mutants in *C. albicans* (Appendix). Solid mediums tested at 16ºC, 30ºC, and 37ºC against include: 5mM and 10 mM H_2O_2, 8 mM and 16 mM SPD, SLAD, M199 pH 7.5 and 4.5, YNBAA pH 5.6 and 6.8, YNBAA + Lactate pH 5.6 and 6.8, YNBAA + glucose pH 6.8, YNBAA + NH_4 pH 5.6 and 6.8, YPD + Caffeine, Lee's, M. Lee's, SPIDER. We did not find any medium nor temperature that allowed us to identify a phenotype for *C. glabrata agp*2Δ. Altogether, these results suggest a clear involvement of Agp2 in the sensitivity of *C. glabrata* to KM29, however, no specific phenotype for *C. glabrata agp*2Δ was identified.

Deletion of *C. glabrata LAM1* gene.

The procedure for the deletion of *LAM1* was the same as the one carried out for the deletion of *AGP2*. The first step was the design of the guide RNA primers, cloning into pV1382

and sequencing of the plasmid. A repair template was designed by overlapping primers extended by PCR. Once the plasmid was obtained it was used to transform *C. glabrata* CBS 138 with and without repair template. Figure 12 shows the results of the transformation, indicating a clear enrichment in the colonies obtained when the repair template was present, generating approximately 26 large colonies and 150 small colonies. In contrast, the plate without repair template produced approximately 2 large colonies and 60 small colonies. We are currently confirming the *lam1*Δ mutants by PCR and the positive mutants will be confirmed by DNA sequencing. The characterization of the *lam1*Δ mutant will be as shown earlier for the *agp*2Δ mutant, including susceptibility to KM29 and characterization of additional phenotypes based on phenotypes described for *lam1*Δ and *sip3*Δ in *S. cerevisiae*.

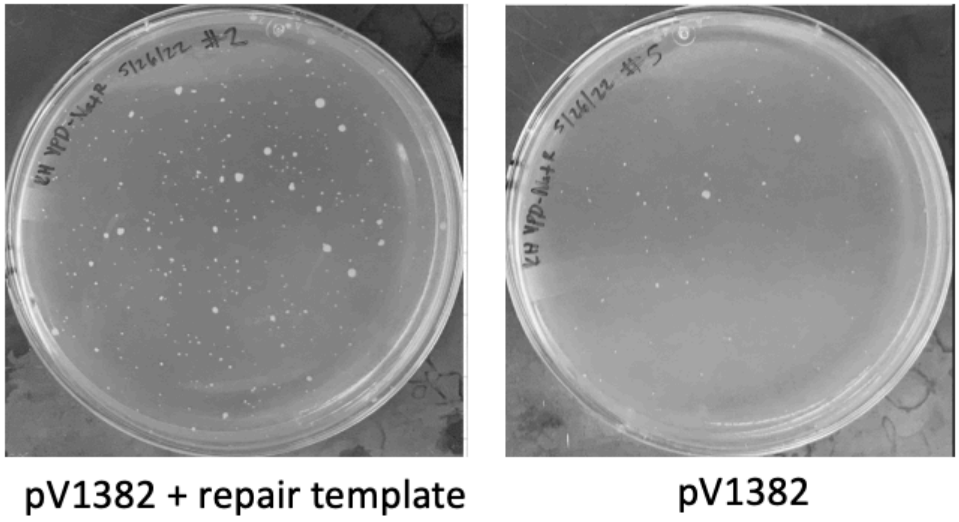

Figure 12: *Candida glabrata lam1*Δ transformation results.

DISCUSSION

The goal of this work was to identify genes and pathways in *C. glabrata* that would provide a framework for understating the mechanism of action of a novel antifungal peptide, KM29. This effort is a continuation of the initial characterization of gene deletions that caused increased resistance to KM29, identified in a screen devised for the whole-genome haploid deletion collection in *S. cerevisiae* (Bullock et al 2020). The objective was to use the findings of the genomic screen in *S. cerevisiae* as a blueprint to study the effect of mutations in the homologous genes in *C. glabrata* with relation to the fungicidal activity of KM29. Hypothetically, mutations in genes that increase KM29 resistance would unravel genes or processes involved in KM29 cellular uptake and killing. The variety of genes and functions identified in the screen suggests that KM29 may enter the cell through multiple independent transport systems. We focused on plasma membrane transporters belonging to four general groups: hexose transport (*HXT2*, *HXT3*, *HXT5*, and *HXT10*), metal transport (*FET4* and *ZRT2)*, polyamine transport (*AGP2*), and sterol transport (*LAM1* and *SIP3)*. Validation of the increased resistance provided by deletions of these genes was determined by KM29 killing microdilution assays using the original *S. cerevisiae* strains from the deletion library. We did not find significant differences in the yeast survival to KM29 treatment between the *hxt* mutants and the wild-type strain, and similar results were obtained with the metal transporters. Considering the redundancy of genes involved in hexose transport, it would be interesting to test the effect of a combined deletion in multiple transporters, since at least *hxt3*Δ showed a mild increase in resistance to KM29. The discrepancy between the screen and the validation data may represent intrinsic differences in the methodology and sensitivity of the assays; the screen was based in a minimum inhibitory concentration (MIC) for yeast growth over 24-48 hours, versus the validation that tested susceptibility to various

concentrations of the peptide during a 2 h period. However, we did confirm increased resistance to KM29 for *agp2*Δ and *sky1*Δ, as well as for *lam1*Δ and *sip3*Δ mutants.

The creation of *AGP2* deletion in *C. glabrata* using CRISPR-Cas9 was successful and proved that a repair template was important to increase the yield during the transformation procedure. It would be interesting to sequence the *AGP2* locus in the colonies that arose without the repair template; this could provide different types of mutants with local changes near the double-strand break site. We did not recognize any sequence changes with respect to the wild-type strains, although some changes were found in the *AGP2* intron region. Two out of three *C. glabrata agp2*Δ strains (independent colonies from the transformation with the *AGP2* guide RNA-Cas9 plasmid) tested displayed increased resistance to KM29. This inconsistency may represent an intrinsic variation in the strain, despite carrying the *agp2*Δ allele. The increased resistance shown by two *agp2*Δ isolates suggests that this gene is likely involved in KM29 function, but further investigation will be required to ascertain its role in *C. glabrata*, which may be different to the function described in *S. cerevisiae*. The lack of resistance to polyamines and the lack of any other phenotype among those tested supports the idea of having a different function. The deletion and characterization of *SKY1* would aid in deciphering the relationship to *AGP2* and overall function of these genes in *C. glabrata*. These findings stress the challenges presented by the limited knowledge of gene function in this yeast.

The deletion of *LAM1* and *SIP3* in *C. glabrata* will provide more information about the gees involved in KM29 function. If they were to increase resistance to KM29 it would suggest that the sterol composition of the plasma membrane would affect KM29 uptake, a hypothesis that can be readily tested by assessing membrane fluidity, sterol content, and KM29 uptake using a fluorescently labeled peptide.

In conclusion, we have established a CRISPR-Cas9 system to delete genes in *C. glabrata* that will allow to test targeted genes and study their effect in killing mechanism of KM29. *AGP2* appears to have an important role in this process, and further experimental work will be required to understand its cellular function and its effect on KM29 fungicidal activity.

REFERENCES

1. Addgene. (2021). *Download Addgene's eBook: CRISPR 101*. Addgene. https://info.addgene.org/download-addgenes-ebook-crispr-101-3rd-edition

2. Akkam, Y. H. (2013). *Design, Development, and Characterization of Novel Antimicrobial Peptides for Pharmaceutical Applications*. ScholarWorks@UARK. https://scholarworks.uark.edu/etd/908/

3. Aouida, M., Leduc, A., Poulin, R., & Ramotar, D. (2005). AGP2 Encodes the Major Permease for High Affinity Polyamine Import in Saccharomyces cerevisiae. *Journal of Biological Chemistry*, *280*(25), 24267–24276. https://doi.org/10.1074/jbc.m503071200

4. Bondaryk, M., Kurzątkowski, W., & Staniszewska, M. (2013). Antifungal agents commonly used in the superficial and mucosal candidiasis treatment: mode of action and resistance development. *Advances in Dermatology and Allergology*, *5*, 293–301. https://doi.org/10.5114/pdia.2013.38358

5. Brachmann CB, Davies A, Cost GJ, Caputo E, Li J, Hieter P, Boeke JD. Designer deletion strains derived from Saccharomyces cerevisiae S288C: a useful set of strains and plasmids for PCR-mediated gene disruption and other applications. Yeast. 1998 Jan 30;14(2):115-32. doi: 10.1002/(SICI)1097-0061(19980130)14:2<115::AID-YEA204>3.0.CO;2-2. PMID: 9483801.

6. Bullock, C. (2018). *Dissecting the Mechanism of Action of a Novel Antifungal Peptide*. ScholarWorks@UARK. https://scholarworks.uark.edu/etd/2891/

7. Bullock, C. B., McNabb, D. S., & Pinto, I. (2020). Whole-Genome Approach to Understanding the Mechanism of Action of a Histatin 5-Derived Peptide. *Antimicrobial Agents and Chemotherapy*, *64*(3). https://doi.org/10.1128/aac.01698-19

8. Camu, B. (2019, March 17). *16 Fascinating Facts About Fungi*. Leaf & Limb. https://www.leaflimb.com/16-Fascinating-Facts-About-Fungi/

9. Candida Genome Database. (2022). *Candida Genome Database*. http://candidagenome.org/cgi-bin/compute/blast_clade.pl

10. Crisprflydesign. (2019). *Supplementary Methods pcfd5 Cloning Protocol*. http://www.crisprflydesign.org/wp-content/uploads/2016/07/pCFD5cloningprotocol.pdf

11. Csank, C., & Haynes, K. (2000). Candida glabrata displays pseudohyphal growth. *FEMS Microbiology Letters*, *189*(1), 115–120. https://doi.org/10.1111/j.1574-6968.2000.tb09216.x

12. de Groot, P. W. J., Kraneveld, E. A., Yin, Q. Y., Dekker, H. L., Groß, U., Crielaard, W., de Koster, C. G., Bader, O., Klis, F. M., & Weig, M. (2008). The Cell Wall of the Human

Pathogen *Candida glabrata* : Differential Incorporation of Novel Adhesin-Like Wall Proteins. *Eukaryotic Cell*, *7*(11), 1951–1964. https://doi.org/10.1128/ec.00284-08

13. Ferraz, L., Sauer, M., Sousa, M. J., & Branduardi, P. (2021). The Plasma Membrane at the Cornerstone Between Flexibility and Adaptability: Implications for Saccharomyces cerevisiae as a Cell Factory. *Frontiers in Microbiology*, *12*. https://doi.org/10.3389/fmicb.2021.715891

14. Gatta, A. T., Wong, L. H., Sere, Y. Y., Calderón-Noreña, D. M., Cockcroft, S., Menon, A. K., & Levine, T. P. (2015). A new family of StART domain proteins at membrane contact sites has a role in ER-PM sterol transport. *eLife*, *4*. https://doi.org/10.7554/elife.07253

15. Ghaddar, N., el Roz, A., Ghssein, G., & Ibrahim, J. N. (2019). Emergence of Vulvovaginal Candidiasis among Lebanese Pregnant Women: Prevalence, Risk Factors, and Species Distribution. *Infectious Diseases in Obstetrics and Gynecology*, *2019*, 1–8. https://doi.org/10.1155/2019/5016810

16. Gournas, C., Athanasopoulos, A., & Sophianopoulou, V. (2018). On the Evolution of Specificity in Members of the Yeast Amino Acid Transporter Family as Parts of Specific Metabolic Pathways. *International Journal of Molecular Sciences*, *19*(5), 1398. https://doi.org/10.3390/ijms19051398

17. Igarashi, K., & Kashiwagi, K. (2000). Polyamines: Mysterious Modulators of Cellular Functions. *Biochemical and Biophysical Research Communications*, *271*(3), 559–564. https://doi.org/10.1006/bbrc.2000.2601

18. *Invasive Candidiasis | Candidiasis | Types of Fungal Diseases | Fungal Diseases | CDC*. (2020). CDC. https://www.cdc.gov/fungal/diseases/candidiasis/invasive/index.html

19. Kavanagh, K., & Dowd, S. (2004). Histatins: antimicrobial peptides with therapeutic potential. *Journal of Pharmacy and Pharmacology*, *56*(3), 285–289. https://doi.org/10.1211/0022357022971

20. Kumar, R., Chadha, S., Saraswat, D., Bajwa, J. S., Li, R. A., Conti, H. R., & Edgerton, M. (2011). Histatin 5 Uptake by Candida albicans Utilizes Polyamine Transporters Dur3 and Dur31 Proteins. *Journal of Biological Chemistry*, *286*(51), 43748–43758. https://doi.org/10.1074/jbc.m111.311175

21. Kumar, T. K. S., McNabb, D. S., Akkam, Y. H., & Nguyen, D. T. (2011). *Peptides with antifungal activity and methods of using the peptides*. ScholarWorks@UARK. https://scholarworks.uark.edu/pat/307/

22. Kurtzman, C. P., Fell, J. W., & Boekhout, T. (2011). *The Yeasts: A Taxonomic Study* (5th ed.) [E-book]. Elsevier Science. eBook ISBN: 9780080931272

23. Labun, K., Montague, T. G., Krause, M., Torres Cleuren, Y. N., Tjeldnes, H., & Valen, E. (2019). CHOPCHOP v3: expanding the CRISPR web toolbox beyond genome editing. *Nucleic Acids Research*, *47*(W1), W171–W174. https://doi.org/10.1093/nar/gkz365

24. Lei, J., Sun, L., Huang, S., Zhu, C., Li, P., He, J., Mackey, V., Coy, D. H., & He, Q. (2019). The antimicrobial peptides and their potential clinical applications. *PubMed Central*, *11*(7), 3919–3931.

25. Mazi, P. B., Olsen, M. A., Stwalley, D., Rauseo, A. M., Ayres, C., Powderly, W. G., & Spec, A. (2022). Attributable Mortality of *Candida* Bloodstream Infections in the Modern Era: A Propensity Score Analysis. *Clinical Infectious Diseases*. https://doi.org/10.1093/cid/ciac004

26. Morgan, J., Meltzer, M. I., Plikaytis, B. D., Sofair, A. N., Huie-White, S., Wilcox, S., Harrison, L. H., Seaberg, E. C., Hajjeh, R. A., & Teutsch, S. M. (2005). Excess Mortality, Hospital Stay, and Cost Due to Candidemia: A Case-Control Study Using Data From Population-Based Candidemia Surveillance. *Infection Control & Hospital Epidemiology*, *26*(6), 540–547. https://doi.org/10.1086/502581

27. Mueller, G. M., Foster, M. S., & Bills, G. F. (2004). *Biodiversity of Fungi: Inventory and Monitoring Methods* (1st ed.) [E-book]. Academic Press. eBook ISBN: 9780080470269

28. Naito, Y., Hino, K., Bono, H., & Ui-Tei, K. (2014). CRISPRdirect: software for designing CRISPR/Cas guide RNA with reduced off-target sites. *Bioinformatics*, *31*(7), 1120–1123. https://doi.org/10.1093/bioinformatics/btu743

29. Neumann, A., Baginski, M., & Czub, J. (2010). How Do Sterols Determine the Antifungal Activity of Amphotericin B? Free Energy of Binding between the Drug and Its Membrane Targets. *Journal of the American Chemical Society*, *132*(51), 18266–18272. https://doi.org/10.1021/ja1074344

30. Norris, H. L., Kumar, R., Ong, C. Y., Xu, D., & Edgerton, M. (2020). Zinc Binding by Histatin 5 Promotes Fungicidal Membrane Disruption in C. albicans and C. glabrata. *Journal of Fungi*, *6*(3), 124. https://doi.org/10.3390/jof6030124

31. Pais, P., Costa, C., Pires, C., Shimizu, K., Chibana, H., & Teixeira, M. C. (2016). Membrane Proteome-Wide Response to the Antifungal Drug Clotrimazole in Candida glabrata: Role of the Transcription Factor CgPdr1 and the Drug:H+ Antiporters CgTpo1_1 and CgTpo1_2. *Molecular & Cellular Proteomics*, *15*(1), 57–72. https://doi.org/10.1074/mcp.m114.045344

32. Perea, S., & Patterson, T. (2002). Antifungal Resistance in Pathogenic Fungi. *Clinical Infectious Diseases*, *35*(9), 1073–1080. https://doi.org/10.1086/344058

33. R AN, Rafiq NB. Candidiasis. [Updated 2022 Feb 24]. In: StatPearls [Internet]. Treasure Island (FL): StatPearls Publishing; 2022 Jan-. Available from: https://www.ncbi.nlm.nih.gov/books/NBK560624/?report=classic

34. Raschmanová, H., Weninger, A., Glieder, A., Kovar, K., & Vogl, T. (2018). Implementing CRISPR-Cas technologies in conventional and non-conventional yeasts: Current state and future prospects. *Biotechnology Advances*, *36*(3), 641–665. https://doi.org/10.1016/j.biotechadv.2018.01.006

35. *Reverse Complement*. (2022). Reverse Compliment. https://www.bioinformatics.org/sms/rev_comp.html

36. Roetzer, A., Gabaldón, T., & Schüller, C. (2010). From Saccharomyces cerevisiae to Candida glabrata in a few easy steps: important adaptations for an opportunistic pathogen. *FEMS Microbiology Letters*, *314*(1), 1–9. https://doi.org/10.1111/j.1574-6968.2010.02102.x

37. Schwarzmüller, T., Ma, B., Hiller, E., Istel, F., Tscherner, M., Brunke, S., Ames, L., Firon, A., Green, B., Cabral, V., Marcet-Houben, M., Jacobsen, I. D., Quintin, J., Seider, K., Frohner, I., Glaser, W., Jungwirth, H., Bachellier-Bassi, S., Chauvel, M., . . . Kuchler, K. (2014). Systematic Phenotyping of a Large-Scale Candida glabrata Deletion Collection Reveals Novel Antifungal Tolerance Genes. *PLoS Pathogens*, *10*(6), e1004211. https://doi.org/10.1371/journal.ppat.1004211

38. Sites, J. N. (2018). The Role of Plasma Membrane Transporters in the Antifungal Activity of a Novel Peptide. *ScholarWorks*.

39. Synthego. (2022). *The Complete Guide to Understanding CRISPR sgRNA*. https://www.synthego.com/guide/how-to-use-crispr/sgrna

40. Tati, S., Jang, W. S., Li, R., Kumar, R., Puri, S., & Edgerton, M. (2013). Histatin 5 Resistance of Candida glabrata Can Be Reversed by Insertion of Candida albicans Polyamine Transporter-Encoding Genes DUR3 and DUR31. *PLoS ONE*, *8*(4), e61480. https://doi.org/10.1371/journal.pone.0061480

41. Ueno, K., Uno, J., Nakayama, H., Sasamoto, K., Mikami, Y., & Chibana, H. (2007). Development of a Highly Efficient Gene Targeting System Induced by Transient Repression of *YKU80* Expression in *Candida glabrata*. *Eukaryotic Cell*, *6*(7), 1239–1247. https://doi.org/10.1128/ec.00414-06

42. Vyas, V. K., Barrasa, M. I., & Fink, G. R. (2015). A Candida albicans CRISPR system permits genetic engineering of essential genes and gene families. *Science Advances*, *1*(3). https://doi.org/10.1126/sciadv.1500248

43. Vyas, V. K., Bushkin, G. G., Bernstein, D. A., Getz, M. A., Sewastianik, M., Barrasa, M. I., Bartel, D. P., & Fink, G. R. (2018). New CRISPR Mutagenesis Strategies Reveal Variation in Repair Mechanisms among Fungi. *mSphere*, *3*(2). https://doi.org/10.1128/msphere.00154-18